

2020



Paderborn University - Fachgebiet
Theoretische Elektrotechnik



Electromagnetic simulation of the optical response of gold triangular nanoprism: The effect of dielectric substrate

Master's Project
at the Department of Theoretische Elektrotechnik
Prof. Dr. rer. nat. Jens Förstner

Submitted by : Shoukath Ali Mohammad, Hala Fares
Matriculation number : 6819945, 6772271
Branch : Electrical Systems Engineering
Supervisor : Dr. Viktor Myroshnychenko
Examiner : Prof. Dr. rer. nat. Jens Förstner

Contents

List of Figures	v
1. Introduction	1
1.1. Nanoparticles and their properties	1
1.2. Surface plasmon resonances(SPR) and metal nanoparticles	3
1.2.1. Surface Plasmon Polaritons (SPP)	4
1.2.2. Localized Surface Plasmon Resonances (LSPR) in metal nanoparticles	4
1.2.3. SPP Vs LSPR	5
1.3. Applications of nanoparticles	6
2. Methods and Tools	8
2.1. Finite Element Method (FEM)	8
2.2. COMSOL Multiphysics Software	9
2.3. Calculation of optical properties	11
2.3.1. Near- and far-fields	13
2.3.2. Extinction, scattering, and absorption cross-sections	13
3. Results and Discussion	15
3.1. Gold (Au) triangular nanoprism	15
3.2. Optical properties of self-supporting Au nanoprisms(Model1)	16
3.2.1. Different methods of scattering cross-section calculation	27
3.3. Au nanoprisms on semi-infinite dielectric substrate(Model2)	28
3.4. Absorption Cross-Section Vs Scattering Cross-Section	40
3.5. Effect of substrate on the resonant frequency	41
4. Conclusion and Future work	42
A. Appendix	43
Bibliography	47

List of Figures

1.1. Different structures and colours of Au nanoparticles	2
1.2. Middle-age plasmonic engineering,(a) Lycurgus cup(British Museum London),(b) Sainte Chapelle (Paris)	3
1.3. Surface plasmon polariton on the surface of the metal nanoparticle .	4
1.4. Localized surface plasmon resonance	5
1.5. Application area of nanoparticles	6
1.6. Silicon photovoltaic cells with gold nano-islands embedded in p–n junctions	7
2.1. Basic process of building FE Model	8
2.2. Steps to perform a finite element analysis in COMSOL Multiphysics	9
2.3. Scattering and absorption in a sphere	14
3.1. Gold (Au) triangular nanoprism	15
3.2. The real and the imaginary parts of the relative permittivity of gold	16
3.3. Plane of excitation- Self-supporting Au nanoprism	17
3.4. Meshed model of self-supporting Au nanoprism in a spherical PML	18
3.5. Self-supporting Au nanoprism, length: 50nm	19
3.6. Self-supporting Au nanoprism, length: 75nm	20
3.7. Self-supporting Au nanoprism, length: 100nm	21
3.8. Self-supporting Au nanoprism, length: 150nm	23
3.9. Self-supporting Au nanoprism, length: 200nm	24
3.10. Self-supporting Au nanoprism, length: 250nm	26
3.11. Different methods of SCS calculation	27
3.12. Model of Au nanoprism with semi-infinite substrate	30
3.13. Degenerate mode-Au nanoprism	31
3.14. Comparing model1 with model2, length: 50nm	32
3.15. Comparing model1 with model2, length: 75nm	33
3.16. Comparing model1 with model2, length: 100nm	34
3.17. Comparing model1 with model2, length: 150nm	35
3.18. Comparing model1 with model2, length: 200nm	37
3.19. Comparing model1 with model2, length: 250nm	39
3.20. ACS Vs SCS	40
3.21. Effect of substrate on resonant frequency of Au nanoprism of different sizes	41

1. Introduction

Nanoparticles are minute structures which include small substances of at least one dimension less than 100nm [1]. They bridge the bulk materials with the molecular structures. They also have a large surface area to volume ratio which reduces the melting temperature of nanoparticles and makes them more reactive to other molecules. The researchers found that shape of the nanoparticle influences the properties of a substance for example optical properties. These shapes can be 0D, 1D, 2D or 3D [2].

Figure 1.1 shows the different structures of Au nanoparticles. Dreaden et al.[3] pointed out that nanoparticles, when synthesized with different sizes and shapes, showed different characteristic colours and properties utilized in biometric applications. The modification of the size, nanoshell thickness or the gold concentration the absorption properties of the nanoparticles can be influenced and due to these, different colours of observation can be obtained. Nanoparticles have a tiny size and a large surface area. So, they are suitable for various applications. Due to their optical properties, they have special importance in photocatalytic applications. In spite of the wide application of Nanoparticles, they have drawbacks too. Scientists should pay attention to health hazards caused by ungovernable use of nanoparticles and their discharge in the natural environment.

The objective of this project is to study the Optical cross section spectra such as Absorption Cross-Section (ACS), Scattering Cross-Section (SCS) and Extinction Cross-Section (ECS) of a self-supporting gold triangular nanoprism and nanoprism with semi-infinite silica substrate as a function of size of the nanoprism on the spectra, plot the near and far-field of the particle. the size of the nanoprism is changed by varying the length of the nanoprism side from 50[nm]to 250[nm] this NP is excited by plane wave with wavelength ranging from 400nm to 1000nm. In this chapter the nanoparticle in general, its properties and applications will be discussed. In chapter two we briefly introduce the COMSOL software and explain the finite element method. In the third chapter we discuss the results of the simulation and analyze them. Finally we will conclude the project and provide some incites for the future work.

1.1. Nanoparticles and their properties

Nanoparticles dependet on their properties, shapes or sizes are classified into different classes[4]. (fullerenes, metal nanoparticles , ceramic nanoparticles , and polymeric nanoparticles). Nanoparticles have unique physical and chemical prop-

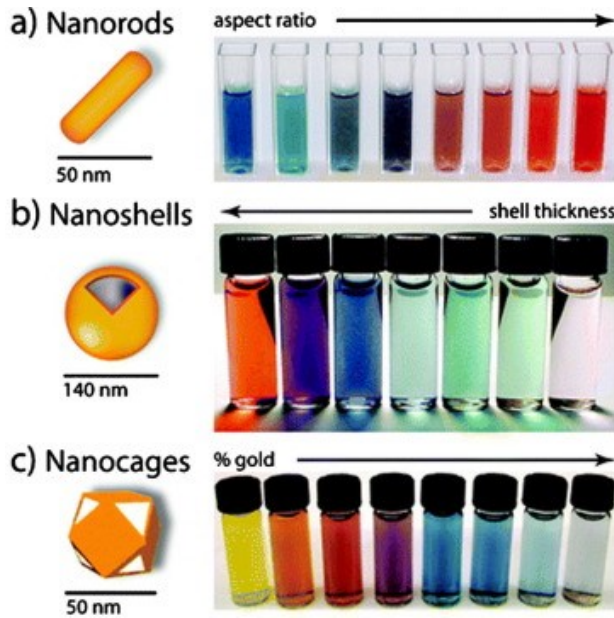


Figure 1.1.: Different structures and colours of Au nanoparticles[3]

erties because of their high surface area and nanoscale size.

Carbon-based nanoparticles: carbon-based nanoparticles have two major classes fullerenes and carbon nanotubess (CNTs), they have become a special commercial interest due to their electrical conductivity, high strength, structure, electron affinity, and versatility[5].

Ceramics nanoparticles: Ceramics nanoparticles are inorganic nonmetallic solids they have a special importance because they can be used in many different applications such as catalysis, photocatalysis, photodegradation of dyes, and imaging applications[6]

Semiconductor nanoparticles: They have properties between metals and nanometals and due to these properties they found many applications in the literature[7].

Polymeric nanoparticles: These are organic based nanoparticles and are readily functonlized and due to this they have many applications in literature[8][9]..

Lipid-based nanoparticles: These particles contain lipid moieties and they are used in many biomedical applications[10].

Metal nanoparticles: Metal nanoparticle are made from metals and have unique optoelectrical properties due to Localized Surface Plasmon Resonance (LSPR) characteristics. Gold nanoparticles are one example of metal nanoparticles which are used in many research applications. Advantages of using gold nanoparticle is that it is an inert metal, it does not oxidize, so no complicated calculation of optical properties caused by oxide layers. Furthermore it shows strong optical response in the visible region of the electromagnetic spectrum, not in the ultraviolet (UV) region like many other metals. Changing resonance in gold nanoparticle causes visible changes in colour. Finally, many different shapes and sizes of gold nanoparticles can be used due to new synthesis methods[11]. Because of the advantages of gold

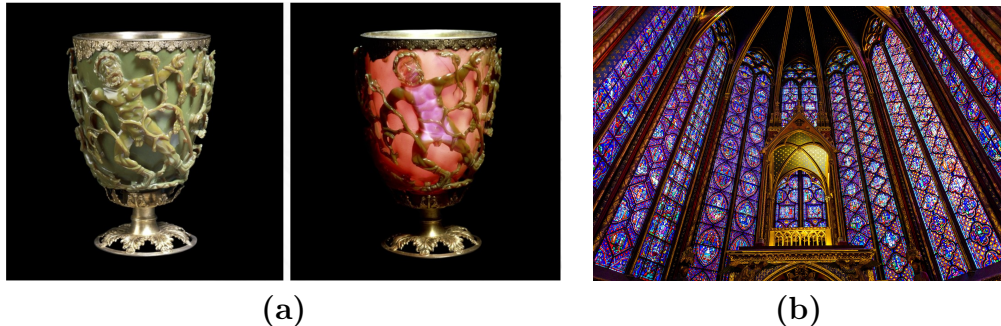


Figure 1.2.: Middle-age plasmonic engineering,(a) Lycurgus cup(British Museum London)[12], London), (b) Sainte Chapelle (Paris)[13]

nanoparticles compared to other nanoparticles we use gold triangular nanoprisms in this project.

Metal nanoparticles are suitable for use in many applications due to their electromagnetic and optical properties [10]. some of the most important property are:

Electronic and optical properties : the optical properties of metal nanostructures were used in the past by the artists to create brilliant colors[Figure 1.2]. For example by inserting different sizes of gold nanoparticle into the glass, group of colors are generated. Nowadays scientists are interested in the electromagnetic properties of metal–dielectric interfaces. The frame of classical Maxwell equations describe the interaction of the electromagnetic fields with metals. The optical and electronic properties of nanoparticles are inter-dependent to greater extent. For instance, noble metals nanoparticles have size dependent optical properties and exhibit a strong UV–visible extinction band that is not present in the spectrum of the bulk metal[10].

Magnetic properties: The best size for the nanoparticle to achieve a best performance is between 10-20 nm[14] because at this size the magnetic properties of nanoparticles dominate effectively. The distribution of electrons in nanoparticles leads to magnetic property.

1.2. Surface plasmon resonances(SPR) and metal nanoparticles

The free electrons which appear on the surface of the metal can oscillate due to their interaction with the electric field. When a light-beam is incident on an obstacle the oscillated charges are known as plasmons[15]. These plasmons oscillate with the same frequency of the material's surface. As a condition for this is that the incident light frequency must be equivalent to the natural frequency of the material (in our project the material is gold(Au)). This phenomenon is called as surface plasmon resonance (SPR).

1.2.1. Surface Plasmon Polaritons (SPP)

A surface plasmon polariton (SPP) is an electromagnetic excitation that propagates in a wave along the planar interface between a metal and a dielectric medium; usually vacuum, whose electromagnetic field declines exponentially with distance from the surface and due to this decline, the electromagnetic field of a surface plasmon polariton can not be observed in (far-field) experiments till the SPP is transformed into light. The electromagnetic field of a surface plasmon polariton at a dielectric–metal interface is derived by the solution of Maxwell's equation, which have to be separately solved for the metal and dielectric part[16].

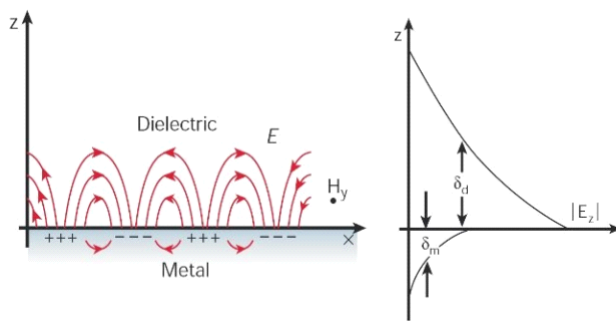


Figure 1.3.: Surface plasmon polariton on the surface of the metal nanoparticle[17]

Polariton and its relation with skin depth. In Figure1.3, $|E|$ is the z-component of plane wave which decays exponentially with characteristic length δ_d . The $l\delta_d$ represents the skin depth of electric field component in dielectric while δ_m represents the skin depth in metal.

1.2.2. Localized Surface Plasmon Resonances (LSPR) in metal nanoparticles

LSPR is an optical event created by light when it comes in contact with conductive nanoparticles; The nanoparticles are lesser than the incident wavelength. The electric field of incident light can be utilized to excite electrons of a conduction band, ending in oscillations with a resonant frequency that almost entirely depends on the composition, size, geometry and separation distance of nanoparticles. Nanoparticles with its complete properties can be defined in the RF Module which is provided by COMSOL Multiphysics environment and LSPR can be visualized on the surface of nanoparticles when excited by an electric field.

The Figure1.4(c) above is nearfield plot. The hot spots indicate the excitation of the plasmons in the direction of the electric field for a resonant frequency.

Figure1.4(b) shows how as a light wave passes through a material, the induced electric field creates a charge separation in the atoms, creating an electron cloud that then allows for electrons to move freely.

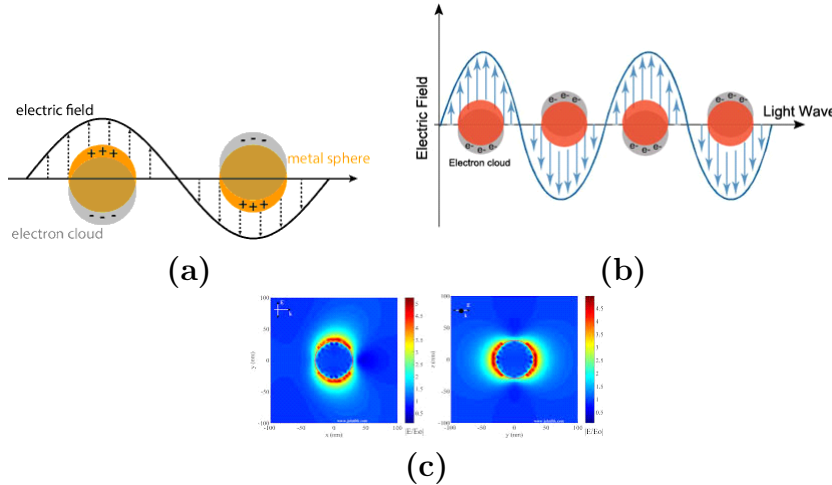


Figure 1.4.: (a)Phenomenon of Localized Surface Plasmon Resonance[18], (b)Basics of localized surface plasmon resonance (LSPR) of gold nanoparticles due to collective oscillation of surface electrons with incident light at a specific wavelength[19], (c)Simulation of localized surface plasmon resonance[20]

The collective response of conduction electrons control the optical properties of gold nanoparticles in the visible and near-infrared (vis-NIR). When a light field incident on electron gas this will move from its stable position due to that surface polarization charges will be induced and act as a reconstruct force on the electron gas. Both the near and far-field response of gold nanoparticles are strongly effected by plasmons. Far-field is an important term for the discuss of the absorption and scattering while near-field affect the ambient of the particle[11]. As mentioned above electromagnetic waves (light) incident on a plasmon (metal-dielectric surface) excite oscillating charges due to the interact of the electric field of the em wave with the charges on the surface of the particle. The incidental electromagnetic waves can be scattered on the surface of the particle in all directions or absorbed and converted to another form of energy "thermal energy" by the oscillating charges[21].

1.2.3. SPP Vs LSPR

Figure1.3 and Figure1.4(a) shows the difference between SPP and LSP. In the case of surface plasmon polaritons, plasmons propagate in the x and y-directions along the metal-dielectric interface, for distances on the order of tens to hundreds of microns, and decline in the z-direction. For the case of localized surface plasmons, light interacts with particles much smaller than the incident wavelength (Figure1.4(a)). This leads to a plasmon that oscillates locally around the nanoparticle with a frequency known as the LSPR.

1.3. Applications of nanoparticles

Nanoparticles are used in many applications due to all the important properties mentioned earlier. Some of the applications are:

- Applications in drugs and medications:** Nanoparticles can be used to diagnose and treat cancer due to their SPR. When a light incident on an Au nanoparticle, it absorbs the light and convert it into heat which can be exploited in the thermal therapy of cancer[22]. Furthermore, nanoparticles are able to increase the therapeutic efficiency of the drugs, weaken the side effects and improve the patient compliance by using their ability to deliver drugs in the typical dose.
- Applications in manufacturing and materials:** Nanotechnology is desired in many industries implying food processing and packing. Furthermore, they are used in many chemical sensors and biosensors application because of their plasmon absorbance features. The resonance wavelength is strongly influenced on shape and size of NPs, the interparticle distance and the dielectric property of the ambient medium.

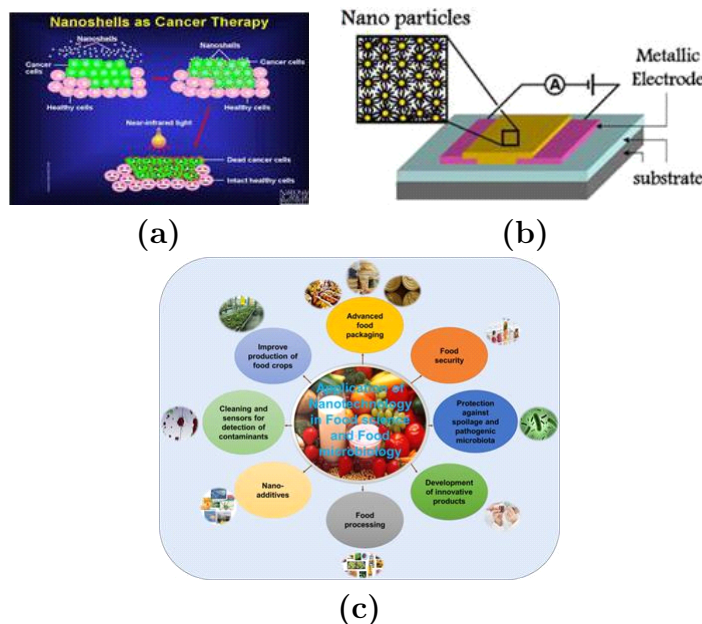


Figure 1.5.: Application area of nanoparticles in (a) treatment of cancer[23], (b) pressure sensor[24], (c) food science[25]

Applications in electronics: Nanoparticle electronics can be used to create big digital displays which have a high electricity-efficient, bright in color, and its manufacture does not cost much.

Applications in mechanical industries: Nanoparticles deliver many applications in mechanical industries especially in coating, lubricants and adhesive applications. Furthermore, this property helps to achieve mechanically stronger nanodevices for many targets.

Application in solar cells: Solar cells are good alternative energy sources but are not widely used due to their high cost and low efficiency. The efficiency of the

solar cells can be increased by using gold nano-islands embedded in semiconductor junction. The solar batteries made from nanoparticles have longer life. For example 12v nanoparticle batteries have a 10 year service and 2v nanoparticles batteries have 15 year.

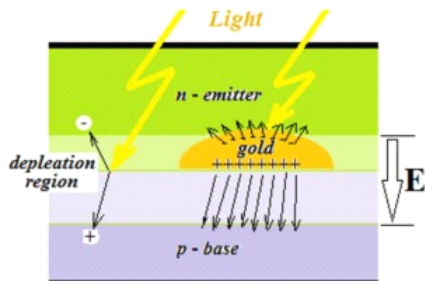


Figure 1.6.: Silicon photovoltaic cells with gold nano-islands embedded in p-n junctions[26]

And many other applications in medicine, food, electronics, fuel and solar cells, batteries, aerospace technology, fuels, cleaner air and water, sensors, fabric and much more.

2. Methods and Tools

2.1. Finite Element Method (FEM)

Finite Element Method (FEM) is powerful application and plays an important role in solving engineering problems and mathematical analysis. Typical problem areas of interest include heat flow, elastic, fluid flow, mass transport and electrostatics, electromagnetics and optics. FEM is numerical method, used to solve the “approximate” solutions to boundary value problems of partial differential equations. This method divided the structures into several smaller domains or in the pieces of structure by creating a “mesh” followed by reconnecting all the sub-divided elements by means of “nodes” which holds all the discretized elements together. This process of sub-division is called discretization which results in a set of simultaneous algebraic equations. The advantage of using this method that its flexibility in selection of discretization for the various shaped elements (e.g. triangular, rectangular, tetrahedral) which is need to be discretize space and the basis functions [27]. Another basic feature of FEM is the usage of boundary conditions for finding solution. The finding of only “approximate” solutions to the problems falls under drawbacks of this method.

Here in this project, commercial software “COMSOL 5.4” is used for building a FE Model. The flow chart below defines the typical procedure followed by any commercial software.

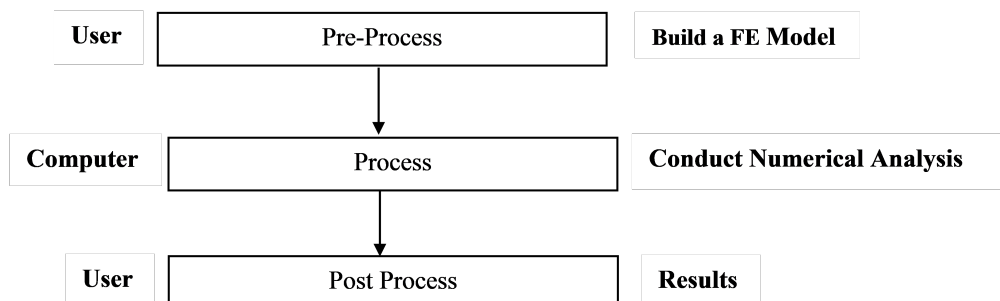


Figure 2.1.: Basic process of building FE Model

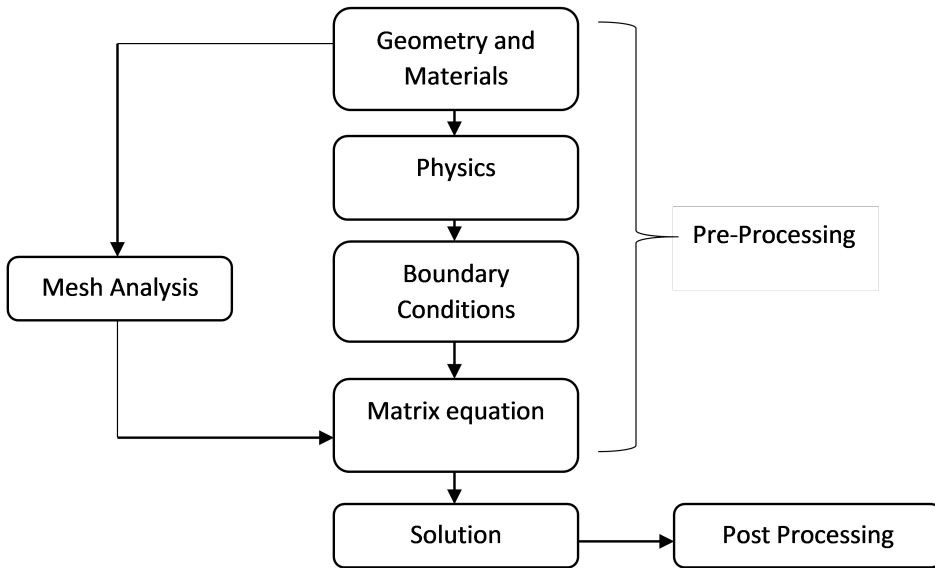


Figure 2.2.: Steps to perform a finite element analysis in COMSOL Multiphysics[30]

2.2. COMSOL Multiphysics Software

"COMSOL Multiphysics is a cross-platform finite element analysis, solver and multiphysics simulation software. It allows conventional physics-based user interfaces and coupled systems of partial differential equations (PDEs)"[28]. It also has wide range of application areas i.e. Acoustics, Bioscience, Radio frequency components, Semiconductor Devices, Optics, Photonics etc. It mainly emphasizes on the Finite Element Method to solve various models in the field of engineering, physics and chemistry. COMSOL Multiphysics works on the 1D, 2D and 3D objects problems. Here in this project, three-dimensional triangular gold nanoparticle is used for the computation. COMSOL Multiphysics can be used in many application areas because Partial Differential Equations form the basis for the laws of sciences and provide the foundation for modelling a wide range of scientific and engineering phenomena [29]. Acoustic module, MEMS module, AC/DC module, Radio Frequency module, Heat Transfer Module etc. are their optional modules. Here, Radio Frequency modules has been used for the electromagnetic simulation of the optical response of gold triangular prism nanoparticles. The Finite Element Analysis (method to study phenomenon in relation to FEM) in COMSOL Multiphysics followed a procedural flow as shown in the Figure 2.2.

This method is divided into three basics steps: pre-processing, solver and post processing. Model is built by the user in the pre-processing process. Pre-processing process is divided into smaller sub-steps for better understanding of the FEM applications. Firstly, creation of interconnected geometry (in our case is 3D) to represent the domain under study and assign the material properties to the do-

main. The modeling of the geometry is done by CAD tool. Then, the physical environments of the problem under investigation are generated by assigning the underlying physics (or multiphysics), mathematical equations, and finite element formulation to the model [30]. After that mesh is created which divides the complete geometry into smaller parts and computation is done by software into subdivided parts followed by boundary and initial conditions to the domain under study as well as its discretization into finite elements, determine the matrix equation governing the model [30]. The post processing steps allow us to evaluate the results by means of plotting the graph.

The electromagnetics equations available in COMSOL are applied on specific models to analyse the behaviour of particles. In this project, differential form of Maxwell's equation has been used to analyse the electromagnetic behaviour in Radio Frequency Module. Maxwell's equation for the time-varying field can be written as:

$$\text{rot } \vec{H}(\vec{r}, t) = \partial_t \vec{D}(\vec{r}, t) + \vec{J}(\vec{r}, t) \quad (2.1)$$

$$\text{rot } \vec{E}(\vec{r}, t) = -\partial_t \vec{B}(\vec{r}, t) \quad (2.2)$$

$$\text{div } \vec{B}(\vec{r}, t) = 0 \quad (2.3)$$

$$\text{div } \vec{D}(\vec{r}, t) = \rho(\vec{r}, t) \quad (2.4)$$

Where \mathbf{J} and ρ are the macroscopic current and charges.

Maxwell's equation at interfaces between the two media with \vec{n}_{12} normal vector for an electric field and magnetic field is given by:

$$(\vec{E}_1 - \vec{E}_2) \times \vec{n}_{12} = 0 \quad (2.5)$$

$$(\vec{B}_1 - \vec{B}_2) \cdot \vec{n}_{12} = 0 \quad (2.6)$$

Equation 2.5 and 2.6 defines that tangential component of electric field strength and normal component of magnetic flux density across the interfaces is continuous, whereas the magnetic field strength and electric flux density between two media can be expressed as

$$(\vec{H}_1 - \vec{H}_2) \times \vec{n}_{12} = j_s \quad (2.7)$$

$$(\vec{D}_1 - \vec{D}_2) \cdot \vec{n}_{12} = \sigma_s \quad (2.8)$$

where j_s and σ_s is the surface current density and surface charge between the media respectively. For j_s and $\sigma_s = 0$, we can say that tangential component of magnetic field strength and normal component of electric flux density across the interfaces is continuous.

Maxwell's equation can also be expressed in terms of harmonic time dependence. Replacing time derivative by $\partial t \rightarrow j\omega$, we may rewrite equation 2.1 to 2.4 as

$$\text{rot } \vec{H}(\vec{r}, \omega) = j\omega \vec{D}(\vec{r}, \omega) + \vec{J}(\vec{r}, \omega) \quad (2.9)$$

$$\text{rot } \vec{E}(\vec{r}, \omega) = -j\omega \vec{B}(\vec{r}, \omega) \quad (2.10)$$

$$\text{div } \vec{B}(\vec{r}, \omega) = 0 \quad (2.11)$$

$$\text{div } \vec{D}(\vec{r}, \omega) = \rho(\vec{r}, \omega) \quad (2.12)$$

By solving equation 2.9 and 2.10, “**wave electric equation**” can be expressed as

$$\nabla \times (\mu^{-1} \nabla \times \vec{E}) - k_0^2 \epsilon_{rc} \vec{E} = 0 \quad (2.13)$$

k_0 and ϵ_{rc} are wave number and complex relative permittivity respectively and it is defined as $k_0 = \frac{\omega}{c_0}$ and $\epsilon_{rc} = \epsilon'_r + j\epsilon''_r$. Here

$$\begin{aligned} \epsilon'_r &= n^2 - k^2 \\ \epsilon''_r &= 2nk \end{aligned} \quad (2.14)$$

where c_0 , n and k represent speed of the light, complex refractive index and damping factor of the electromagnetic wave respectively.

The RF modules of COMSOL Multiphysics offer different boundary condition such as absorbing boundary conditions, scattering boundary conditions and port boundary conditions. The radiation in the scattered field, diverted from the source which cannot be classified as plane wave with particular direction of propagation. It is also required to apply boundary conditions in radiation problems. Perfectly Matched Layer (PML) is an option as an additional domain, not boundary condition added to exterior of the model which absorbs incident radiation without producing any reflections [31]. On the other hand, scattering boundary conditions stops the reflections for outgoing wave by making boundary transparent. Generally, PML domain gives more accurate solutions in frequency domain compared to time domain. Therefore, scattering boundary condition is the appropriate choice to work in frequency domain.

2.3. Calculation of optical properties

Scattering is a physical process in which the forms of lights, sound, electromagnetic field (EM) wave etc. deviates from a plane trajectory to one or more paths due to non-uniform properties of the medium through which they pass. Scattering of EM waves by the nanoparticles can be discussed by two concepts: Rayleigh scattering which is generally applied for small, dielectric and non-absorbing particles and on the other hand Mie Scattering is useful for providing a general solution to the scattering solutions without any limitation to the size of the nanoparticles. In this project, we have considered the Mie concept and noticed that the resonance of

scattering amplitude is directly dependent on the sizes of the triangular gold nano particles. The greater the size of the particles, more will be the scattered light moving in the forward direction.

From equations 2.15, we can define the total wave of decomposition into incident and scattered wave.

$$\begin{aligned}\vec{E} &= \vec{E}_{inc} + \vec{E}_{sca} \\ \vec{H} &= \vec{H}_{inc} + \vec{H}_{sca}\end{aligned}\quad (2.15)$$

where \vec{E}_{inc} , \vec{E}_{sca} , \vec{H}_{inc} , \vec{H}_{sca} are the Incident Electric Field, Scattered Electric Field, Incident Magnetic Field and Scattered Magnetic Field respectively.

From Faradays law of electromagnetic equation and Maxwell's wave equation, scattered magnetic field and electric field can be related as:

$$\vec{H}_{sca} = -\frac{1}{j\omega\mu} \nabla \times \vec{H}_{sca} \quad (2.16)$$

$$\nabla \times (\mu_r^{-1} \nabla \times \vec{E}_{sca}) - k_0^2 (\epsilon_r - j \frac{\sigma}{\omega\epsilon_0}) \vec{E}_{sca} = 0 \quad (2.17)$$

From equations 2.16 and 2.17, the calculations of electromagnetic parameters can be easily obtained. In addition to this, time average Poynting vector ($P \frac{w}{m^2}$) describes the direction of the energy flux density can be defined as:

$$P = \frac{1}{2} \times \text{Re}[\vec{E} \times \vec{H}^*] \quad (2.18)$$

The incident component of electric field is related to magnetic field by:

$$\vec{H}_{inc} = \frac{1}{Z} [\hat{k} \times \vec{E}_{inc}] \quad (2.19)$$

where \hat{k} is the direction of incident wave propagation and $Z = \sqrt{\frac{\mu}{\epsilon}}$ is the characteristics impedance. Substituting equation 2.19 in 2.18, the resultant incident Poynting vector is described as:

$$P_{inc} = \frac{1}{2\eta} \times |\vec{E}_{inc}|^2 |\hat{k}| = \frac{1}{2} c \epsilon |\vec{E}_{inc}|^2 |\hat{k}| \quad (2.20)$$

Where c , \hat{k} and $|\vec{E}_{inc}|$ are the speed of light incident light, the permittivity, the direction of the propagating wave, magnitude of the incident electric field respectively.

2.3.1. Near- and far-fields

The near-field and far-field are regions of the EM around a nanoparticle, as a result of radiation scattering of that nanoparticle. The 'near-field' behaviours of electromagnetic fields dominate close to the scattering nanoparticle, while electromagnetic radiation 'far-field' behaviours dominate at greater distances from the nanoparticle. We calculate near-field from normalized electric field as in equation 2.21 and far-field also from the normalized electric field using equation 2.22.

$$normE_{near} = \sqrt{E_{near,x}^2 + E_{near,y}^2 + E_{near,z}^2} \quad (2.21)$$

$$normE_{far} = \sqrt{E_{far,x}^2 + E_{far,y}^2 + E_{far,z}^2} \quad (2.22)$$

2.3.2. Extinction, scattering, and absorption cross-sections

Absorption cross-section σ_{abs} and scattered cross-section σ_{sca} can be related as $\sigma_{abs} = \frac{W_{abs}}{P_{inc}}$ and $\sigma_{sca} = \frac{W_{sca}}{P_{inc}}$ where W_{abs} and W_{sca} are the absorbed electromagnetic energy and scattering electromagnetic energy by the triangular nanoprism respectively. The extinction cross section σ_{ext} can be defined as the amount of energy loss from the incident flux due to absorption and scattering as well as the sum of absorption cross-section and scattering cross-section. By energy balance:

$$\sigma_{ext} = \sigma_{abs} + \sigma_{sca} [m^2] \quad (2.23)$$

The total absorbed energy w.r.t energy loss over the integral volume of the particle can be defined as:

$$W_{abs} = \iiint_{V_p} Q_{loss} dV [W] \quad (2.24)$$

Whereas the energy loss of the particle is given by

$$Q_{loss} = \frac{1}{2} Re[J_{tot} \cdot E^* + j\omega B \cdot H^*] [W/m^3] \quad (2.25)$$

The scattered energy is derived by integrating the scattered irradiance over the imaginary sphere around the particle [21]:

$$W_{sca} = \iint_S P_{sca} \cdot \vec{n} dS [W] \quad (2.26)$$

The optical Theorem states the relation between the total cross-section and the scattering amplitude given by equation 2.27:

$$\sigma_{ext} = \frac{4\pi}{k} lm\{f(0)\}/E_{inc} [m^2] \quad (2.27)$$

Where $f(0)$ is the scattering amplitude in forward direction $\theta = 0^\circ$. COMSOL Multiphysics provide built-in far field calculations for far field parameters 2.27

$$Scattering\ amplitude(E_{far}) = \lim_{r \rightarrow \infty} r E_{sca} \quad (2.28)$$

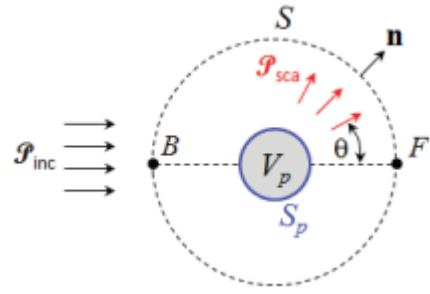


Figure 2.3.: Imaginary sphere, S around a particle of volume, V_p enclosed by surface S_p . Scattering amplitude is evaluated in the forward direction at point F [21]

The extinction cross section can also calculated without the computation of absorption and scattering cross section

$$\sigma_{ext} = \frac{4\pi}{kE_{inc}} lm\{E_{far}(0)\} [m^2] \quad (2.29)$$

3. Results and Discussion

In this chapter we investigate the optical properties of self-supporting Au triangular nanoprisms in air and Au triangular nanoprisms supported on semi-infinite dielectric silica substrate ($\varepsilon_r = 2.25$) as a function of their sizes. In particular, we vary the length of the sides of the triangular nanoprism as seen in Figure 3.1(a). We specifically calculate the linear optical properties of Au nanoprisms such as SCS, ACS and ECS. We also plot the near-field and far-field.

3.1. Gold (Au) triangular nanoprism

For this project we built an Au nanoprism. Figure 3.1 depicts different views of Au nanoprism. The thickness 'T' of the Au nanoprism is fixed to 30nm, the radius

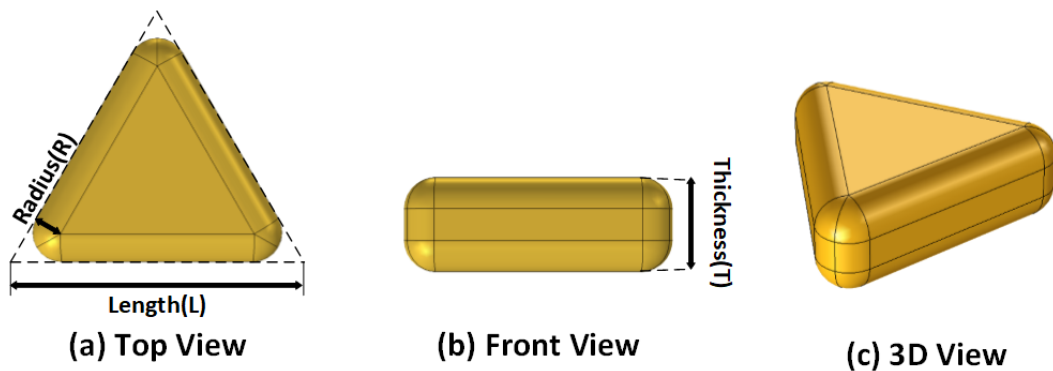


Figure 3.1.: Gold (Au) triangular nanoprism

'R' of the spherical corner of Au nanoprism is fixed to 10nm for all the different sizes of Au nanoprism. The length 'L' of each side of equilateral triangular Au nanoprism is varied as 50nm, 75nm, 100nm, 150nm, 200nm and 250nm to achieve different sizes of nanoprism.

The complex permittivity ε_r of gold is expressed as $\varepsilon_r = \varepsilon' - i\varepsilon''$. The real and imaginary part of the complex permittivity of gold are extracted using the complex refractive index in [32] and then interpolation function is applied and added to the Au nanoprisms in COMSOL. From Figure 3.2 it can be seen that for the desired frequency of 400nm to 1000nm the real part of relative permittivity is negative.

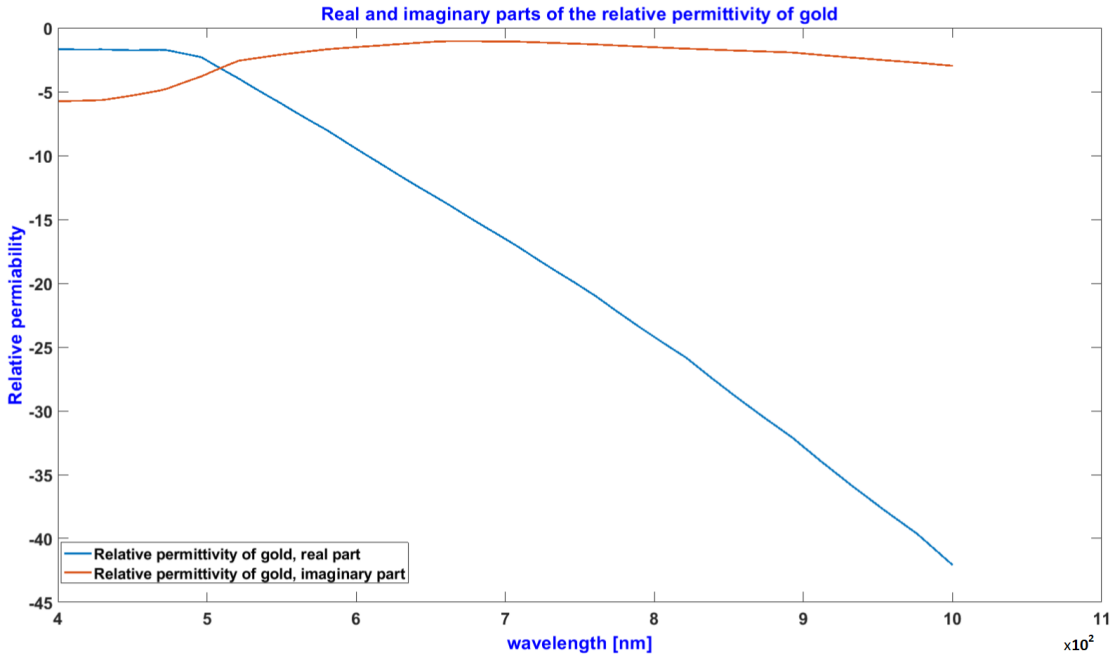


Figure 3.2.: The real and the imaginary parts of the relative permittivity of gold

3.2. Optical properties of self-supporting Au nanoprisms(Model1)

The Au nanoprism of different lengths 'L' were modeled in COMSOL Multiphysics 5.4 software. As we are interested in radio frequency domain we select **Electromagnetic Waves, Frequency Domain (emw)** in the physics tree and then select **Frequency Domain** in the study tree of model wizard. We create a triangle nanoprism of different size using parameters mentioned in section3.1. The nanoprism acts as an Aurum (Au) nanoparticle. We then create a sphere with a reasonable thickness. The sphere acts as a PML. In the **Materials** section we assign air as the material for all domains, except for the nanoprism. We interpolate the real part and the imaginary part of relative permittivity ε_r of gold (Figure 3.2) and define the domain of nanoprism as Au by adding equation 3.1 as a frequency dependent relative permittivity in COMSOL.

$$\varepsilon_r = Au_eps_real(emw.freq) - j * Au_eps_imag(emw.freq) \quad (3.1)$$

where Au_eps_real is the interpolation of the real part and Au_eps_imag is the interpolation of the imaginary part of the complex permittivity of Au.

We apply scattering field solution and excite the model by the plane wave whose components are defined as equation 3.2 in COMSOL, where $E0$ is the magnitude of incident electric field. The plane wave is propagating in negative Z-direction, polarization along x-direction (Figure 3.3). Next we apply **scattering boundary condition** on the outer surface of the PML. This makes sure that the PML outer surface has no effect on the excited plane wave when entering the PML but not

viceversa. The internal PML surface selected for the far-field calculation in the **far-field Domain**.

$$\begin{aligned} Ebx &= E0 * \exp(j * emw.k0 * z) \\ Eby &= 0 \\ Ebz &= 0 \end{aligned} \quad (3.2)$$

where $E0 = 1$ [V/m].

We now apply **mesh** on the model designed so far. By default **free tetrahedral**

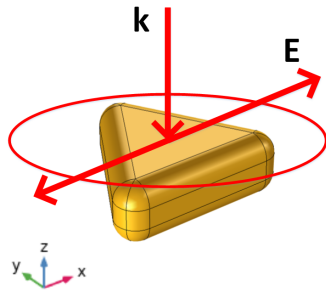


Figure 3.3.: Plane of excitation- Self-supporting Au nanoprism

is applied on the entire model (all triangle shapes in Figure 3.4). We assign the minimum element size of the nanoprism as 1nm and maximum size as 10nm. In general the minimum element size of the rest of the domains is chosen as 1nm and the maximum size as $\lambda/6$, a wavelength dependent parameter. For larger wavelengths the element size increases. We then sweep the entire domain with a distribution of 5 elements. The swept node creates a swept mesh on a domain in 3D by sweeping the mesh from the source face along the domain to an opposite destination face. The distribution node is used to specify the distribution of mesh elements along an edge of a domain. We now add variables to be calculated on the designed model. As we calculate the optical cross-section parameters we define the equations of ACS, SCS, ECS and other parameters required to calculate them in the *Variables* part of **Definitions** section. The ACS is defined as in equation 3.4 where P_{inc} is the incident energy flux and $intop_prism_vol$ is the volume integral of the Au nanoprism. The SCS is calculated using two different methods. One method is on the surface of the nanoparticle as in equation 3.5 where $nrelPoav$ is the relative normal pointing flux (equation 3.3) and $intop_prism_surf$ is the closed surface integral of the surface of the Au nanoprism. The other method is on the internal PML surface as in equation 3.6 where $intop_far_sphere_surf$ is the closed surface integral of the internal PML surface. The difference of two approaches is given in section 3.2.1. The ECS is defined as in equation 3.7.

$$\begin{aligned} nrelPoav &= emw.relPoavx * nx + emw.relPoavy * ny \\ &\quad + emw.relPoavz * nz \quad [W/m^2] \end{aligned} \quad (3.3)$$

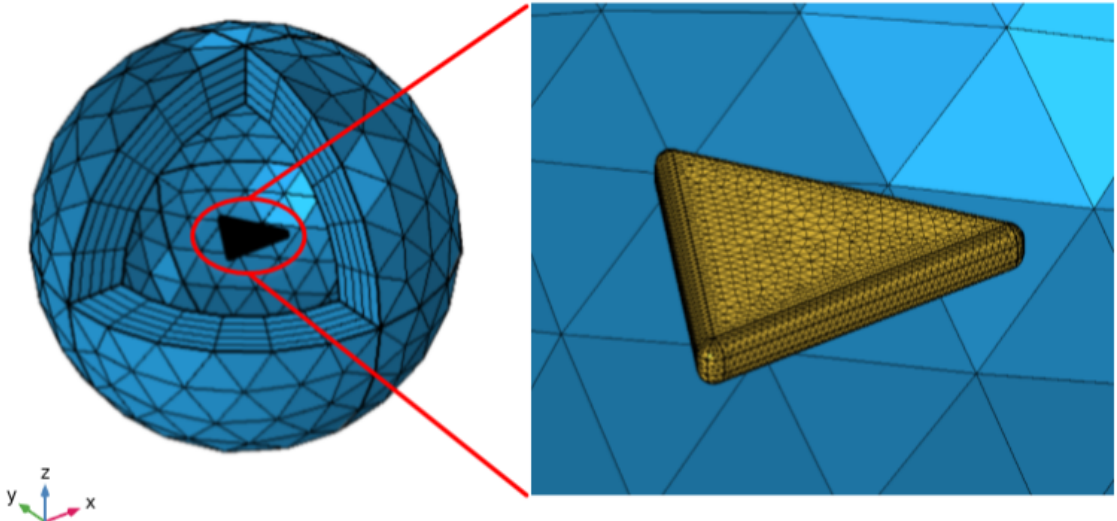


Figure 3.4.: Meshed model of self-supporting Au nanoprism in a spherical PML

$$\sigma_{abs} = \text{intop_prism_vol}(\text{emw.Qh}) / P_{inc} \quad [\text{m}^2] \quad (3.4)$$

$$\sigma_{scs1} = \text{intop_prism_surf}(\text{nrelPoav}) / P_{inc} \quad [\text{m}^2] \quad (3.5)$$

$$\sigma_{scs2} = \text{intop_far_sphere_surf}(\text{nrelPoav}) / P_{inc} \quad [\text{m}^2] \quad (3.6)$$

$$\sigma_{ext} = \sigma_{abs} + \sigma_{scs1} \quad [\text{m}^2] \quad (3.7)$$

where $P_{inc} = 0.5 * E0^2 * c_const * \epsilon_0$ [W/m^2] After defining the cross-section parameters, the effect of the incident field (equation 3.2) on the Au nanoprism in the designed model has to be studied. So, in the **Study** section, in *Parametric Sweep* we select the variable lambda to be varied and vary it from 400nm to 1000nm with a step size of 5nm and compute the study.

After the study is computed we plot the cross-section parameters. To plot the near-field of the normalized electric field, we choose *emw.normE* provided by COMSOL and to plot the far-field, we choose *emw.Efar*. To plot the electric field component along x-direction we choose *emw.Ex*.

Self-supporting Au nanoprism, Length: 50nm

The resonant frequency of the self-supporting Au nanoprism with length 'L' as 50nm was found to be 515nm as seen in Figure 3.5(a). From the plot, it can be observed that absorption dominates scattering because the nanoprism has small surface area and is exposed to a fraction of excitation field. Near-field plot in Figure 3.5(b) shows normalized electric field in xy-plane with strong hot spots on the corners of the nanoprism. Only the sides which are along the polarization direction experienced hot spots. In Figure 3.5(c) the near-field is plotted for the

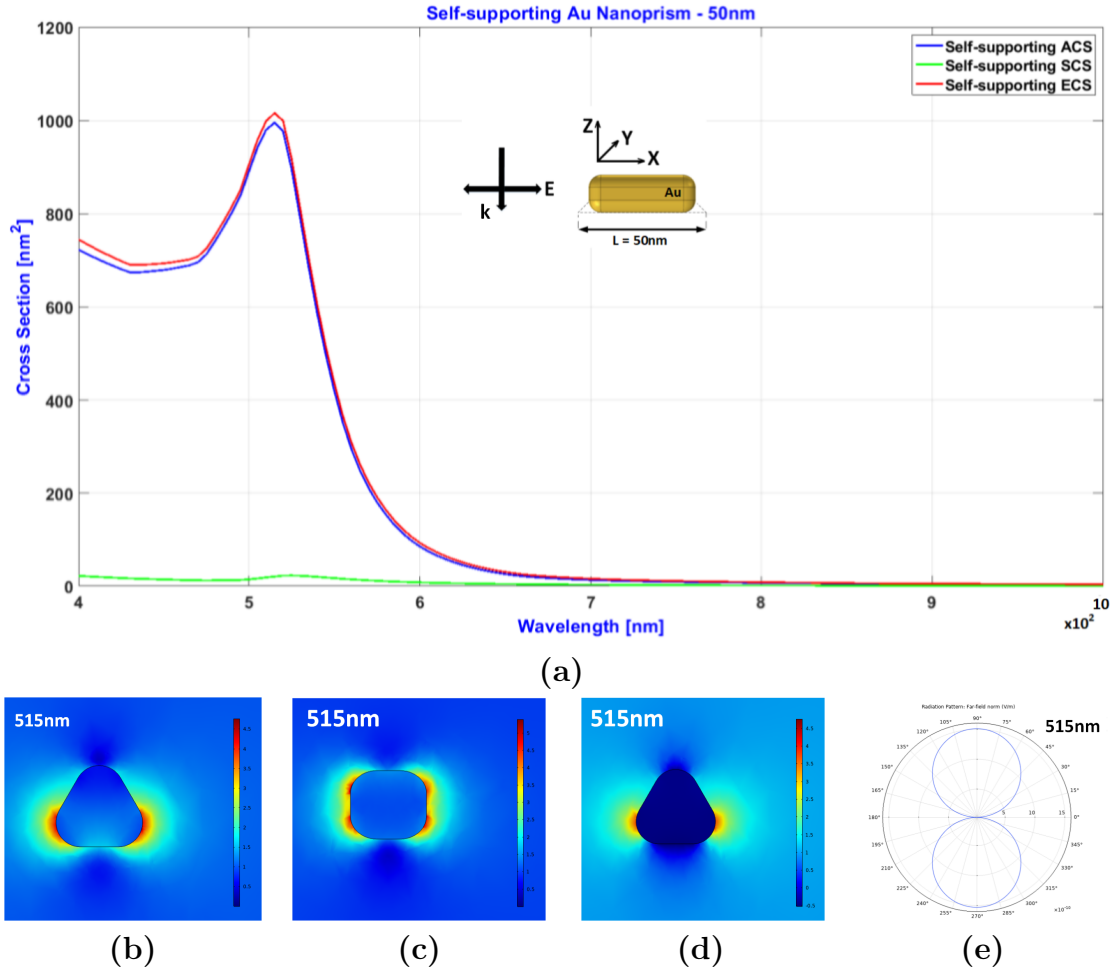


Figure 3.5.: COMSOL numerical results for self-supporting Au nanoprism, length: 50nm; (a) cross-section parameters, (b) near-field plot of normalized electric field in xy-plane, (c) near-field plot of normalized electric field in zx-plane, (d) electric field component E_x in xy-plane (e) far-field showing dipole at 515nm resonant frequency

normalized electric field in the zx-plane. The hot spots can be seen at the corners of the nanoprism similar to the xy-plane. Figure 3.5(d) indicates the electric field component E_x in the xy-plane. The far-field radiation pattern for the wavelength 515nm is plotted in Figure 3.5(e). At the resonant frequency the scattered field

looks similar to the dipole antenna(along zx plane). The blue curve indicates the E-plane containing the electric field polarization and the direction of the maximum radiation.

Self-supporting Au nanoprism, Length: 75nm

The resonant frequency of the self-supporting Au nanoprism with length 'L' as 75nm was found to be 535nm as seen in Figure 3.6(a). From the plot, it can be observed that absorption dominates scattering. Compared to the particle of length 50nm a slight increase in the scattering can be observed due to increase in the surface area. Near-field plot in Figure 3.6(b) shows normalized electric field in xy-

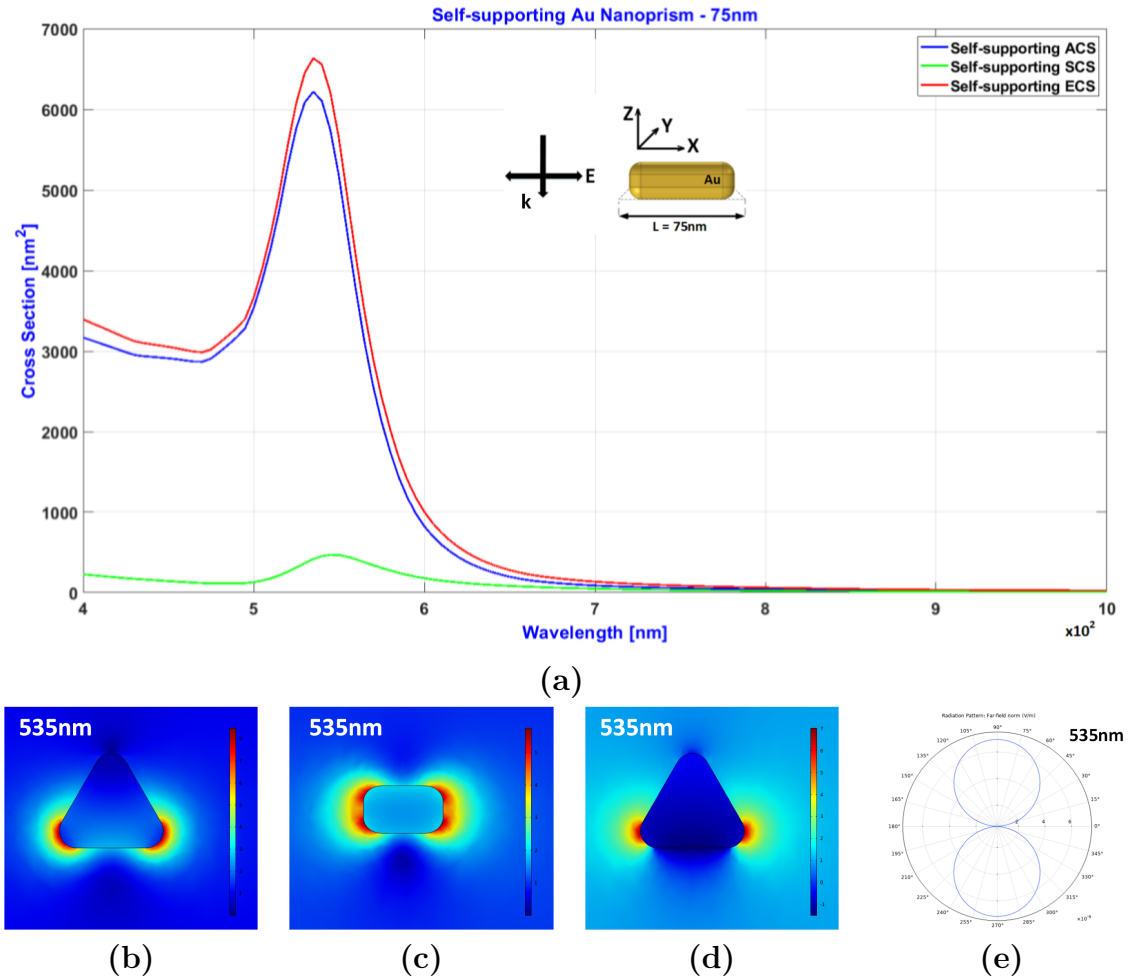


Figure 3.6.: COMSOL numerical results for self-supporting Au nanoprism, length: 75nm; (a) cross-section parameters, (b) near-field plot of normalized electric field in xy-plane, (c) near-field plot of normalized electric field in zx-plane, (d) electric field component E_x in xy-plane, (e) far-field showing dipole at 535nm resonant frequency

plane with strong hot spots on the corners of the nanoprism. Only the sides which

are along the polarization direction experienced hot spots. In Figure 3.6(c) the near-field is plotted for the normalized electric field in the zx-plane. The hot spots can be seen at the corners of the nanoprism similar to the xy-plane. Figure 3.6(d) indicates the electric field component E_x in the xy-plane. The far-field radiation pattern for the wavelength 535nm is plotted in Figure 3.6(e). At the resonant frequency the scattered field looks similar to the dipole antenna(along zx plane). The blue curve indicates the E-plane containing the electric filed polarization and the direction of the maximum radiation.

Self-supporting AU nanoprism, Length: 100nm

The resonant frequency of the self-supporting gold nanoprism with length 'L' as

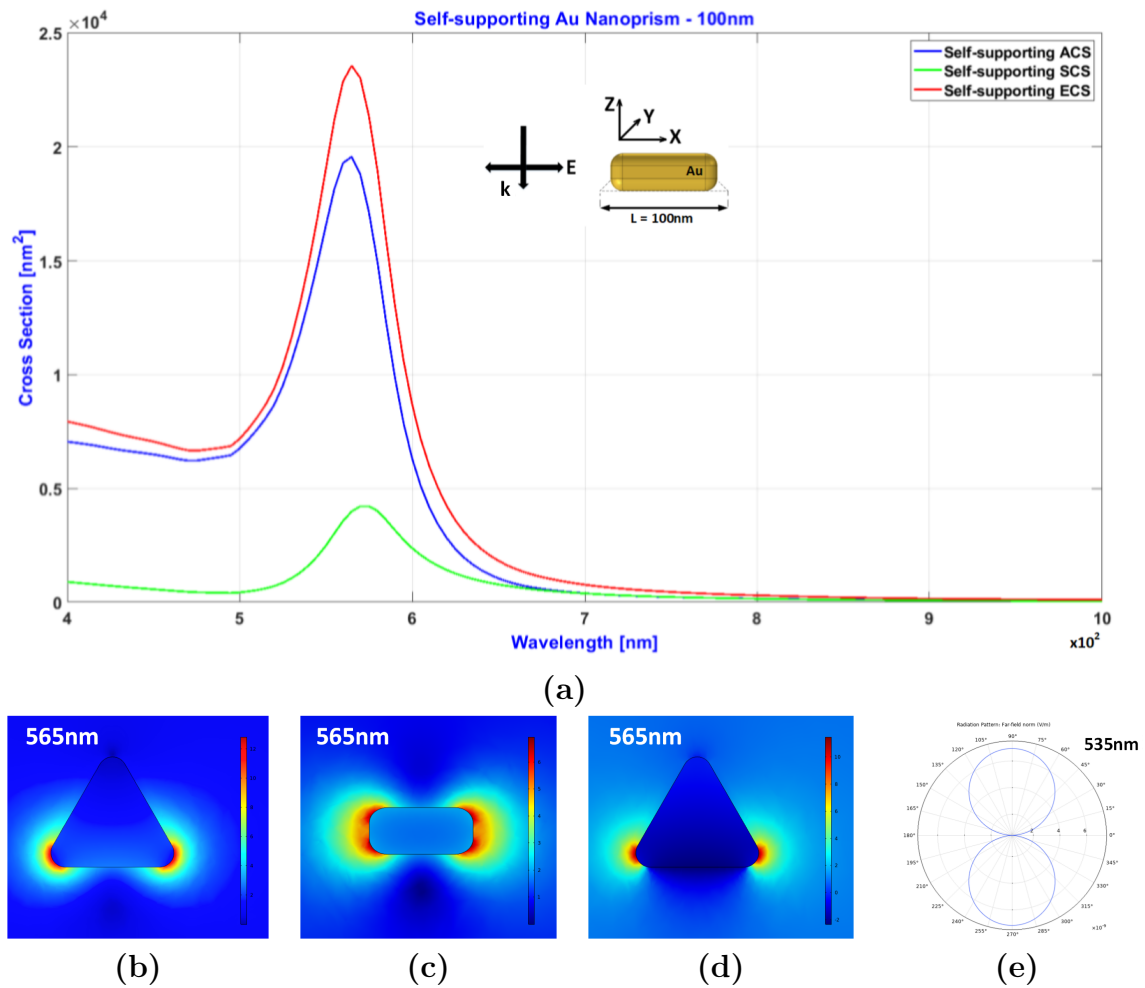


Figure 3.7.: COMSOL numerical results for self-supporting Au nanoprism, length: 100nm; (a) cross-section parameters, (b) near-field plot of normalized electric field in xy-plane, (c) near-field plot of normalized electric field in zx-plane, (d) electric field component E_x in xy-plane, (e) far-field showing dipole at 565nm resonant frequency

100nm was found to be 565nm as seen in Figure 3.7(a). From the plot, it can be observed that absorption dominates scattering. Compared to the particle of length 75nm a slight increase in the scattering can be observed due to increase in the surface area. Near-field plot in Figure 3.7(b) shows normalized electric field in xy-plane with strong hot spots on the corners of the nanoprism. Only the sides which are along the polarization direction experienced hot spots. In Figure 3.7(c) the near-field is plotted for the normalized electric field in the zx-plane. The hot spots can be seen at the corners of the nanoprism similar to the xy-plane. Figure 3.7(d) indicates the electric field component E_x in the xy-plane. The far-field radiation pattern for the wavelength 565nm is plotted in Figure 3.7(e). At the resonant frequency the scattered field looks similar to the dipole antenna(along zx plane). The blue curve indicates the E-plane containing the electric filed polarization and the direction of the maximum radiation.

Self-supporting Au nanoprism, Length: 150nm

The resonant frequency of the self-supporting Au nanoprism with length 'L' as 150nm was found to be 630nm as seen in Figure 3.8(a). From the plot, it can be observed that the scattering cross-section is more compared to the absorption cross-section. In the previous plots ACS has significantly dominated SCS. This is because the surface area of the nanoprism directly exposed to the excited field is large enough to scatter more compared to absorbing the excited field.

Near-field plot in Figure 3.8(b) shows normalized electric field in xy-plane with strong hot spots on the corners of the nanoprism. Only the sides which are along the polarization direction experienced hot spots. In Figure 3.8(c) the near-field is plotted for the normalized electric field in the zx-plane. The hot spots can be seen at the corners of the nanoprism similar to the xy-plane. Figure 3.8(d) indicates the electric field component E_x in the xy-plane. The far-field radiation pattern for the wavelength 630nm is plotted in Figure 3.8(e). At the resonant frequency the scattered field looks similar to the dipole antenna(along zx plane). The blue curve indicates the E-plane containing the electric filed polarization and the direction of the maximum radiation.

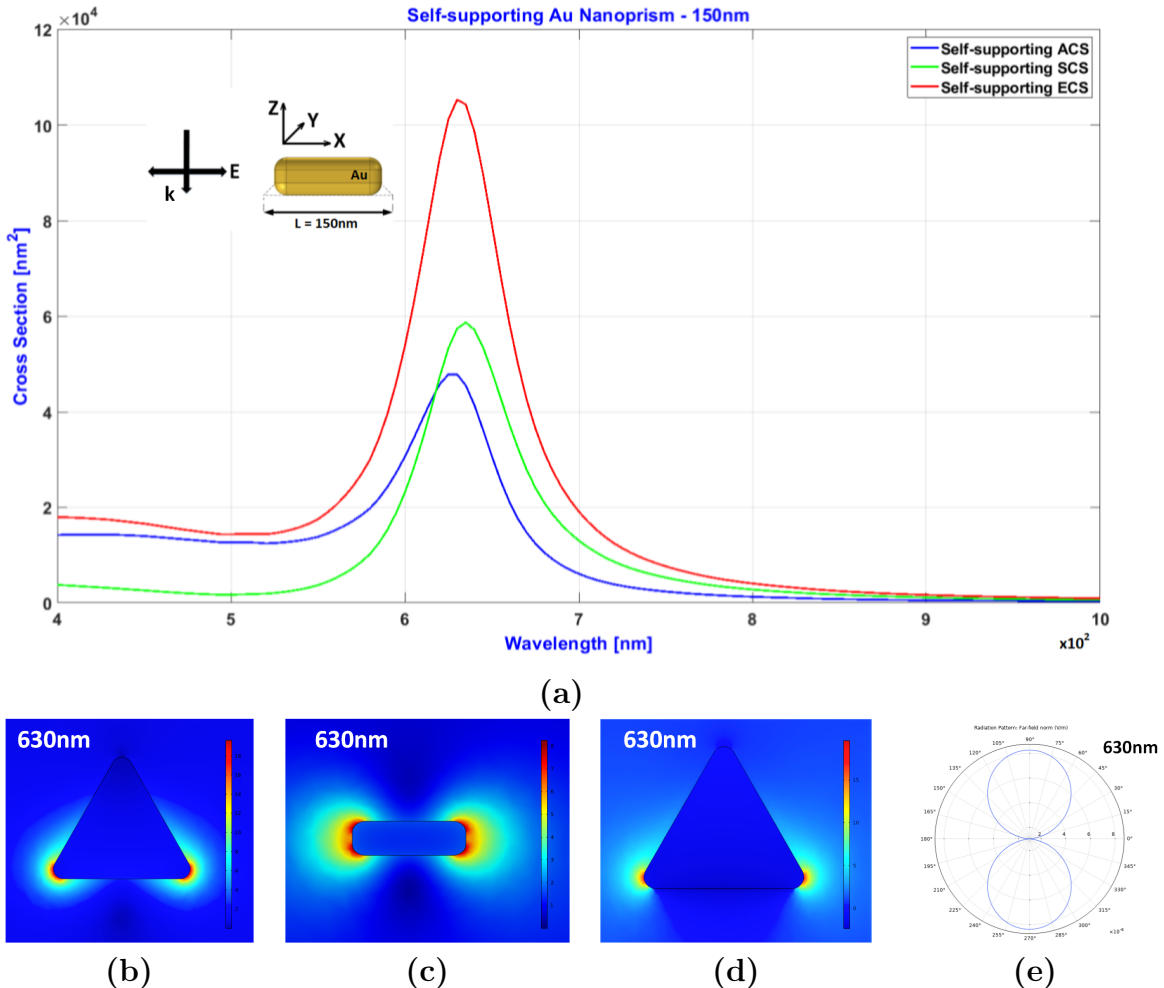


Figure 3.8.: COMSOL numerical results for self-supporting Au nanoprism, length: 150nm; (a) cross-section parameters, (b) near-field plot of normalized electric field in xy-plane, (c) near-field plot of normalized electric field in zx-plane, (d) electric field component E_x in xy-plane, (e) far-field showing dipole at 535nm resonant frequency

Self-supporting Au nanoprism, Length: 200nm

The resonant frequency of the self-supporting gold nanoprism with length 'L' as 200nm was found to be 710nm as seen in Figure 3.9(a). From the plot, it can be observed that SCS completely dominated ACS.

Near-field plot in Figure 3.9(b) shows normalized electric field in xy-plane with strong hot spots on the corners of the nanoprism. Only the sides which are along the polarization direction experienced hot spots. In Figure 3.9(c) the near-field is plotted for the normalized electric field in the zx-plane. The hot spots can be seen at the corners of the nanoprism similar to the xy-plane. Figure 3.9(d) indicates the electric field component E_x in the xy-plane. The far-field radiation pattern for the wavelength 710nm is plotted in Figure 3.9(e). At the resonant frequency the

scattered field looks similar to the dipole antenna(along zx plane). The blue curve indicates the E-plane containing the electric filed polarization and the direction of the maximum radiation.

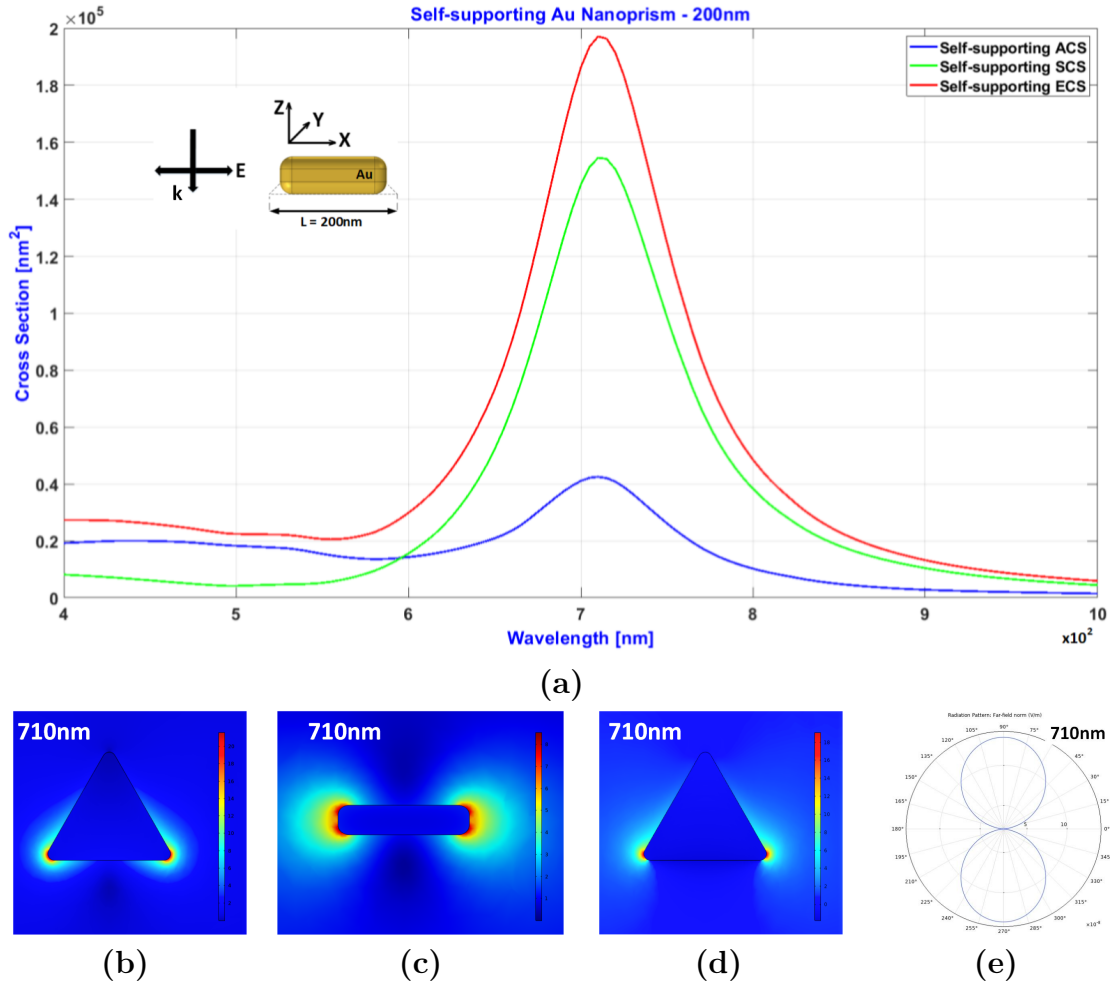


Figure 3.9.: COMSOL numerical results for self-supporting Au nanoprism, length: 200nm; (a) cross-section parameters, (b) near-field plot of normalized electric field in xy-plane, (c) near-field plot of normalized electric field in zx-plane, (d) electric field component E_x in xy-plane, (e) far-field showing dipole at 710nm resonant frequency

Self-supporting Au nanoprism, Length: 250nm

The resonant frequency of the self-supporting gold nanoprism with length 'L' as 250nm was found to be 800nm as seen in Figure 3.10(a). A quadrupolar resonance can be seen at 545nm. From the plot, it can be observed that SCS dominated ACS even more due to the large surface area of the particle.

Near-field plot in Figure 3.10(b) shows normalized electric field in xy-plane with strong hot spots on the corners of the nanoprism. Only the sides which are along the polarization direction experienced hot spots. In Figure 3.10(c) the near-field is plotted for the normalized electric field in the zx-plane. The hot spots can be seen at the corners of the nanoprism similar to the xy-plane. Figure 3.10(d) indicates the electric field component E_x in the xy-plane. The far-field radiation pattern for the wavelength 800nm is plotted in Figure 3.10(e). At the resonant frequency the scattered field looks similar to the dipole antenna(along zx plane). The blue curve indicates the E-plane containing the electric filed polarization and the direction of the maximum radiation.

Figure 3.10(f) shows near-field plot of normalized electric field in xy-plane with strong hot spots on the sides of the nanoprism for the quadrupolar resonance. Unlike the dipolar resonance, the quadrupolar resonance near-field hot spots are on the sides of the nanoprism. In Figure 3.10(g) the near-field is plotted for the normalized electric field in the zx-plane. The hot spots can be seen at the corners of the nanoprism similar which is a perspective view of the xy-plane hot spots. Figure 3.10(h) indicates the electric field component E_x in the xy-plane. The far-field radiation pattern for the wavelength 545nm is plotted in Figure 3.10(e). At the resonant frequency the scattered field looks like a weak resemblance to the quadrupole antenna(along zx plane). The scattering field may strongly resemble to the quadrupole antenna for larger sizes of the nanoprism. The blue curve indicates the E-plane containing the electric filed polarization and the direction of the maximum radiation.

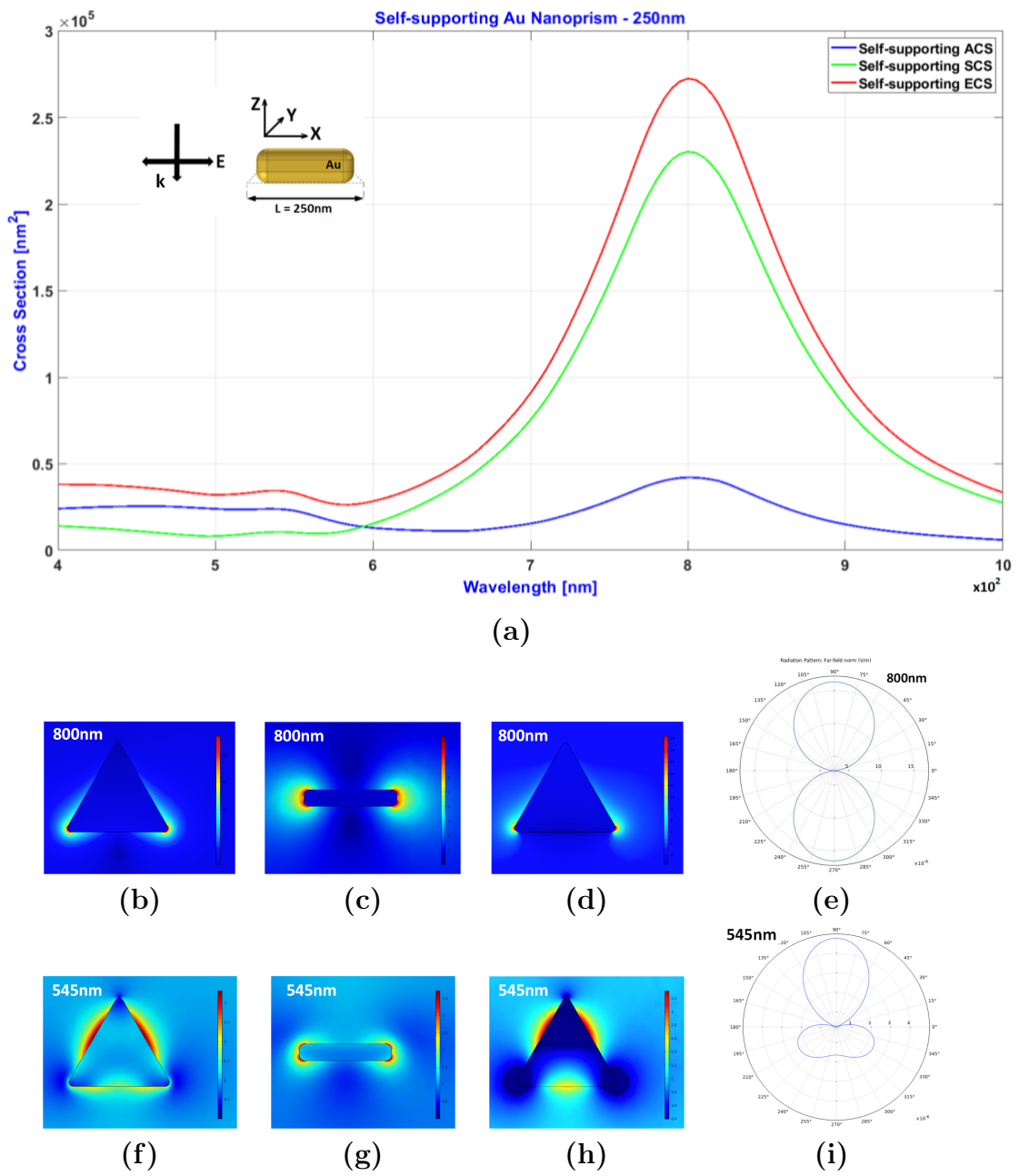


Figure 3.10.: COMSOL numerical results for self-supporting Au nanoprism, length: 250nm; dipolar resonance: (a) cross-section parameters, (b) near-field plot of normalized electric field in xy-plane, (c) near-field plot of normalized electric field in zx-plane, (d) electric field component E_x in xy-plane, (e) far-field showing dipole at 800nm resonant frequency; quadrupolar resonance: (f) near-field plot of normalized electric field in xy-plane, (g) near-field plot of normalized electric field in zx-plane, (h) electric field component E_x in xy-plane, (i) far-field showing dipole at 545nm resonant frequency

3.2.1. Different methods of scattering cross-section calculation

There are two different ways to calculate the SCS of a given nanoparticle. One approach is to calculate SCA on the surface of the nanoparticle(Figure 3.11(b)) using equation 3.5(in COMSOL) and the other approach is to calculate SCS on the surface of the internal PML surface(Figure 3.11(c))(in COMSOL) where all the scattered field is absorbed using equation 3.6. From Figure 3.11(a) it can be seen that both the methods yield similar results.

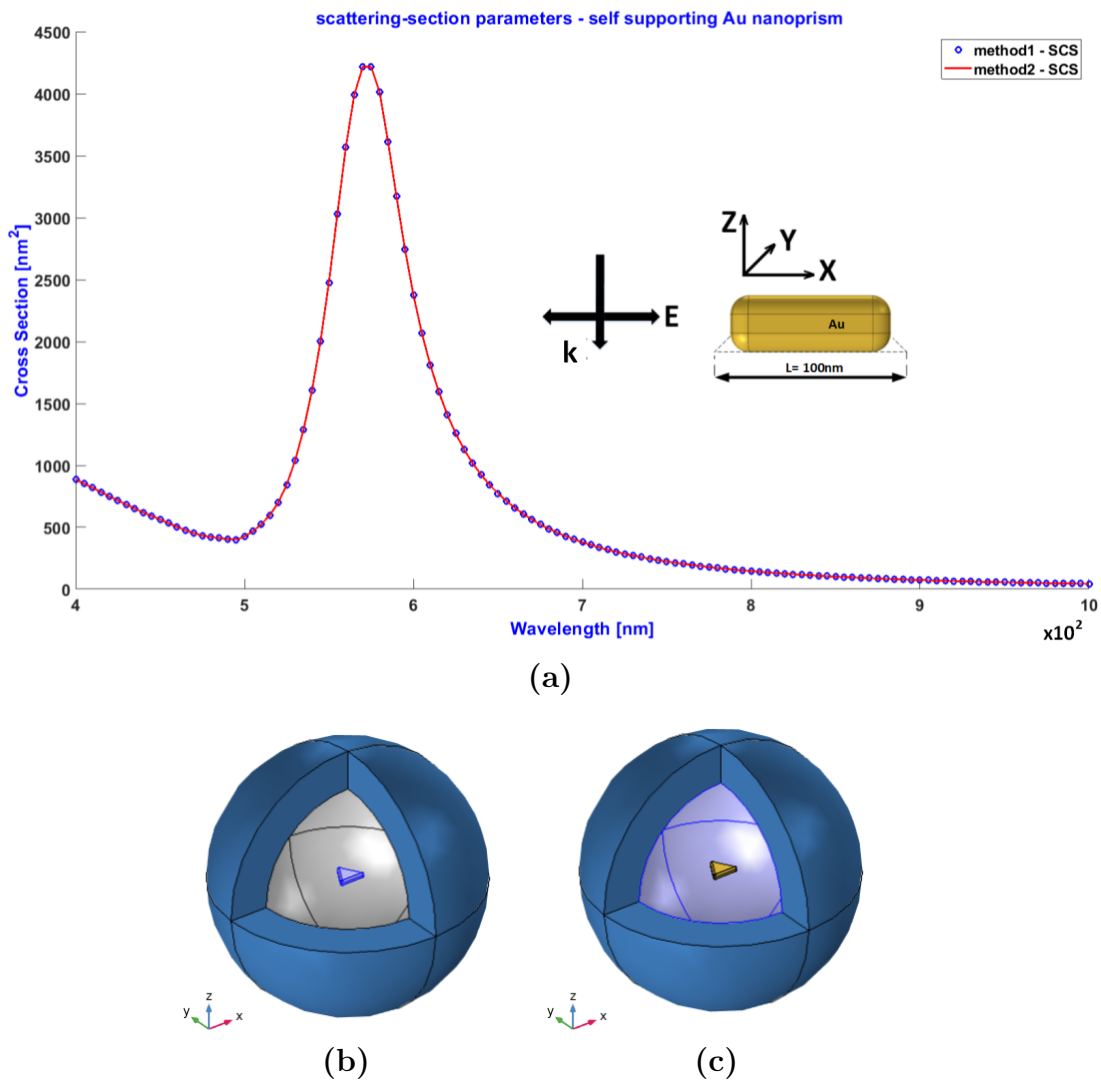


Figure 3.11.: Different methods of SCS calculation, (a) comparison of SCS obtained by two methods, highlighted purple area indicating (b) the particle surface (c) the internal PML surface

3.3. Au nanoprisms on semi-infinite dielectric substrate(Model2)

This model is based on the example model of scatter on substrate provided by COMSOL [33]. The Electromagnetic Waves, Frequency Domain interface features an option to solve for the scattered field, a perturbation to the total field caused by a local scatterer (in our case Au nanoprism). The incident wave is then entered as a background electric field. This field should be a solution to the wave equation without the presence of the scatterer. If the scatterer is suspended in free space or any other homogeneous medium, the background field is simply what is sent into the model. With the scatterer placed on a substrate, the analytical expression for the background field becomes more complicated. It needs to be the correct superposition of an incident and a reflected wave in the free space domain, and a transmitted wave in the substrate.

A simple and general way to avoid deriving and entering the analytical background field is to use a full field solution of the model without the scatterer. To achieve this full field solution, the simulation is set up with two Port conditions. One defines the incident plane wave and allows for specular reflection. The other absorbs the transmitted plane wave. The side boundaries have Floquet conditions, stating that the solution on one side of the geometry equals the solution on the other side multiplied by a complex-valued phase factor.

The propagation direction and the polarization of the incident electric field are input parameters for the periodic ports. Internally, this information is also used by the Floquet conditions. Using the coordinate system in Figure 1, the incident wave vector is

$$\mathbf{k}_a = (k_x, k_y, k_{az}) = k_a (\cos \phi_a \sin \theta_a, \sin \phi_a \sin \theta_a, -\cos \theta_a) \quad (3.8)$$

where k_a is the wave number in the first medium, here vacuum, ϕ_a and θ_a the azimuthal and polar angles of incidence. The expression for the tangentially polarized electric field vector at the plane of incidence becomes

$$\mathbf{E}_0 = E_0 (-\sin \phi_a, \cos \phi_a, 0) \exp (-i (k_x x + k_y y)) \quad (3.9)$$

The Port condition lets you define a total input power from which the electric field amplitude E_0 is derived. The model uses the value

$$P = I_0 A \cos \theta \quad (3.10)$$

where $I_0 = 1MW/m^2$ is the intensity of the incident field and A the area of the boundary where the port is set up. In the substrate, the wave vector is

$$\mathbf{k}_b = (k_x, k_y, k_{bz}) = k_b (\cos \phi_b \sin \theta_b, \sin \phi_b \sin \theta_b, -\cos \theta_b) \quad (3.11)$$

with

$$k_b = \frac{n_b}{n_a} k_a \quad (3.12)$$

$$\phi_b = \phi_a \quad (3.13)$$

$$\sin \theta_b = \frac{n_a}{n_b} \sin \theta_a \quad (3.14)$$

Notice that the x and y components for the wave vector are the same for the wave in the substrate and the incident wave, due to field continuity. The electric field vector at the output port is proportional to

$$(-\sin \theta_b, \cos \theta_b, 0) \exp(-i(k_x x + k_y y))$$

Thus, the mode fields and the mode field amplitudes are the same at the output port as at the input port. A second Electromagnetic Waves, Frequency Domain interface introduces the gold nanoparticle as the scatterer and surrounds the geometry with PMLs. With the full field solution from the first interface as the background field, only the scattered field needs to be absorbed in the PMLs.

The effect of semi-infinite dielectric silica substrate with relative permittivity ($\varepsilon_r = 2.25$) on the Au nanoprism is studied using the model described in Figure 3.12. We follow the same procedure to build the model as explained in section 3.2. We use two Electromagnetic Waves, Frequency Domains (emw and $emw2$) as explained above, emw for full field solution and $emw2$ for scattered field solution. In the mesh the maximum element size of the nanoprism is chosen as 5nm and the maximum element size of substrate is chosen as $\lambda/6/nb$ where $nb = 1.5$ is the refractive index of substrate silica. For the rest of the domains the maximum element size is $\lambda/6$ and the minimum is 0.4nm.

The nanoprism bottom surface is touching the surface of the silica substrate. The silica substrate is cuboid in shape and is surrounded by PML on all the sides including bottom. We used $\theta = 0$ and $\phi = 90$ (in equation 3.9) as one plane of incidence so that electric field propagates in negative z-direction and polarization along x-direction. Other has $\theta = 0$ and $\phi = 0$ (in equation 3.9) as another plane of incidence the electric field propagation in negative z-direction and the polarization along y-direction. We apply equations 3.4, 3.5 and 3.7 to calculate ACS, SCS and ECS respectively by replacing $emw.Qh$ with $emw2.Qh$ to calculate ACS from the scattered field solution.

Degenerate mode

It was observed that the excitation of the two plane waves as explained in the previous section had same effect on the model i.e., both the cases showed similar cross-section patterns as seen in Figure 3.13(a). The degenerate modes plot shown in the Figure 3.13 were plotted for Au nanoprism of side length 100nm. This phenomenon is also called as degenerate mode. Since both the plane waves had similar effect on the cross-section parameters we only consider electric field propagation

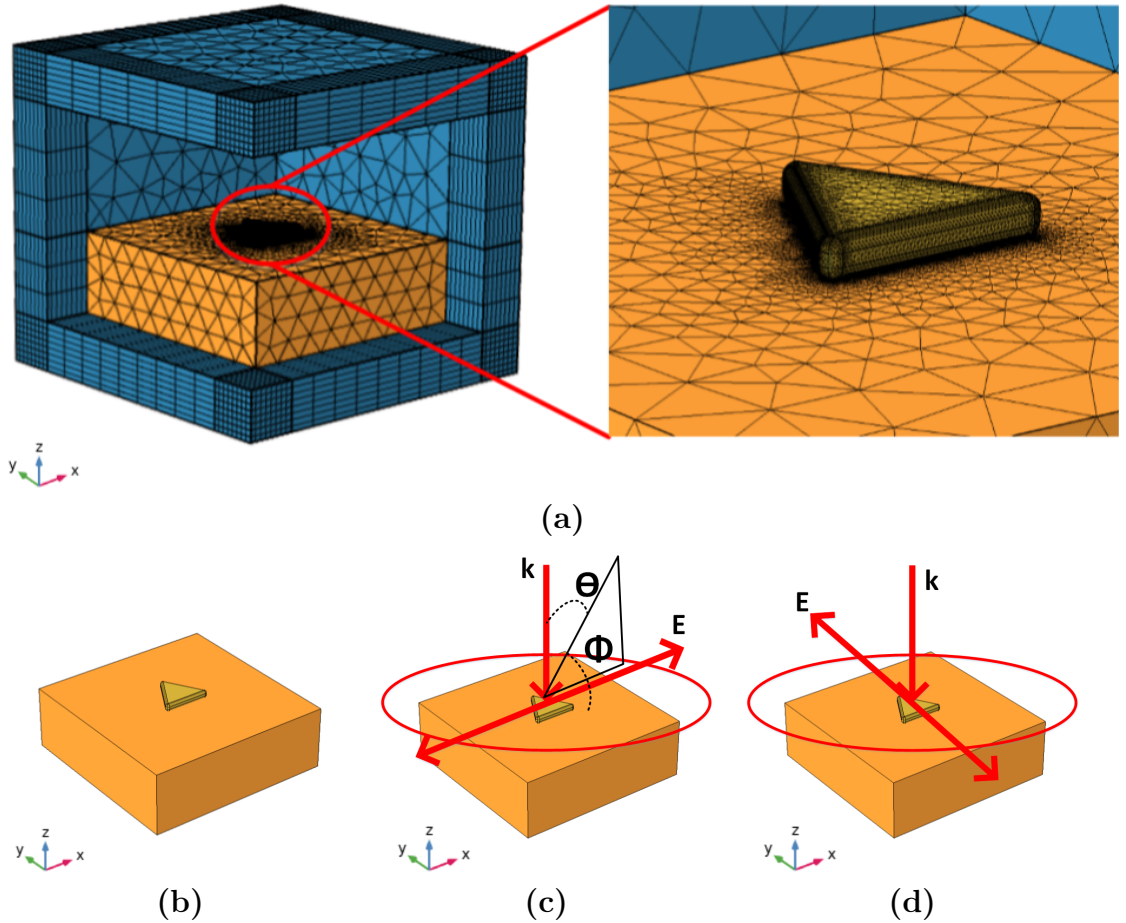


Figure 3.12.: Model of Au nanoprism with semi-infinite substrate, (a) Finely meshed model, (b) highlighted section showing semi-infinite substrate, (c) excitation plane wave 1 where θ is the angle of propagation and ϕ is the angle of polarization, (d) excitation plane wave 2

in negative z-direction and polarization along x-direction similar to the plane wave in self-supporting Au nanoprism model. Near-field plot in Figure 3.13(b) shows normalized electric field of plane wave 1 in xy-plane with strong hot spots on the corners of the nanoprism. Only the sides which are along the polarization direction experienced hot spots. In Figure 3.13(c) the near-field is plotted for the normalized electric field of plane wave 1 in the zx-plane. The hot spots can be seen at the corners of the nanoprism similar to the xy-plane. Figure 3.13(d) indicates the electric field component E_x of plane wave 1 in the xy-plane.

Figure 3.13(e) indicates the near-field plot of the normalized electric field of plane wave 2 in xy-plane. The hot spot can be seen on only one corner which is facing the y-direction as the polarization of plane wave 2 is along y-direction. Figure 3.13(f) and 3.13(g) are the near field plot of normalized electric field in zx-plane and electric field component along xy-plane respectively. From Figure 3.13(b) and

3.13(e) we can notice the difference in the polarization of the plane wave incident on the nanoprism. So, degenerate mode can be noticed from near-field plot.

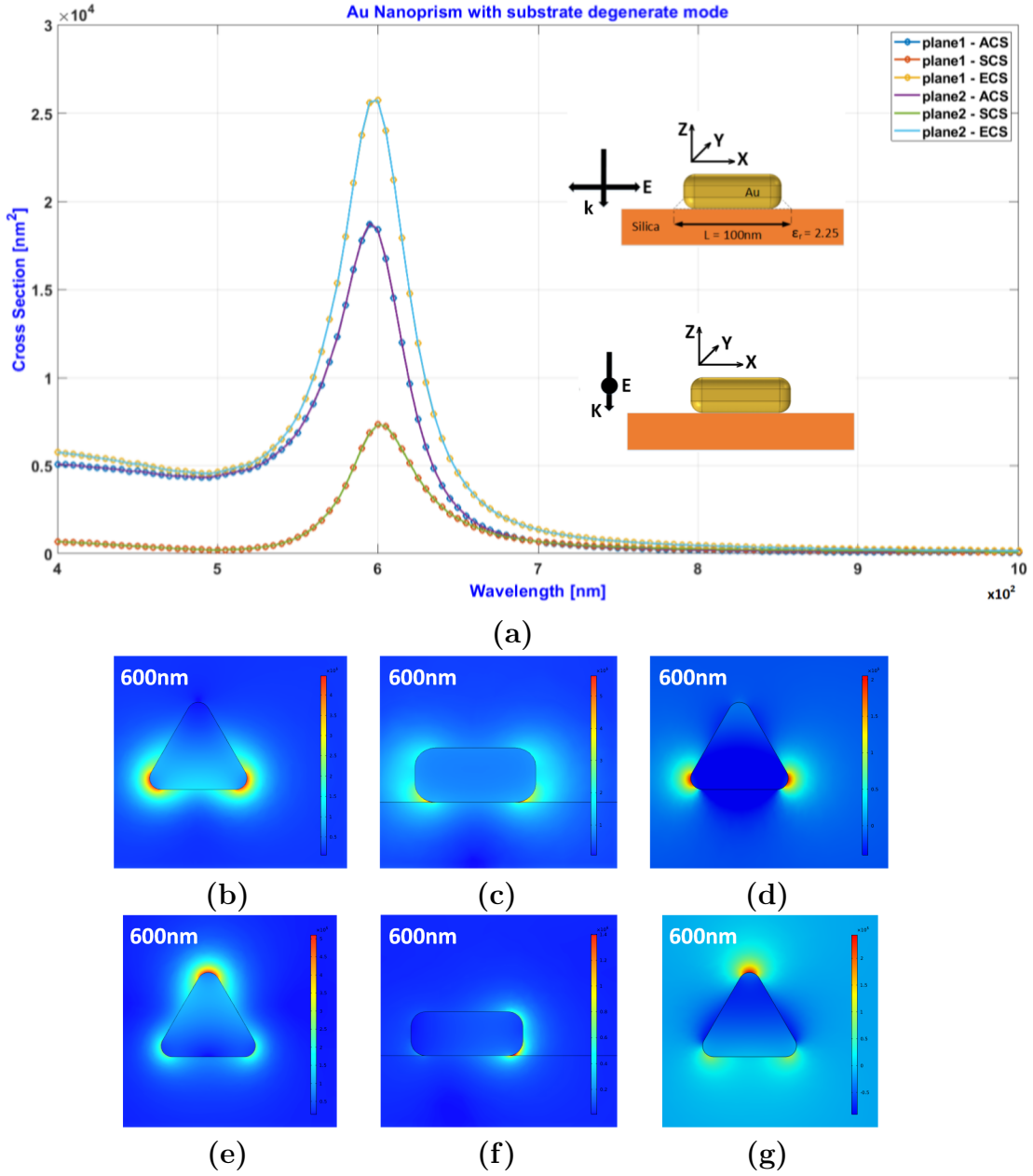


Figure 3.13.: Degenerate mode-Au nanoprism, (a) Cross-section parameters of model2 excited by plane waves with different polarization, one along x-axis and other along y-axis; plane wave 1: (b) near-field plot of normalized electric field in xy-plane, (c) near-field plot of normalized electric field in xz-plane, (d) electric field component E_x in xy-plane; plane wave 2: (e) near-field plot of electric field norm in xy-plane, (f) near-field plot of electric field norm in yz plane, (g) electric field component E_y in xy-plane

Gold nanoprism(50nm) on substrate

From Figure 3.14(a) it can be observed that there is a small shift in the resonant frequency of 5nm from 515nm for self-supporting Au nanoprism model to 520nm for the Au nanoprism with substrate model of length 50nm. This shift in frequency depicts the effect of substrate on the Au particle. Near-field plot in Figure 3.14(b) shows normalized electric field in xy-plane with strong hot spots on the corners of the nanoprism. Only the sides which are along the polarization direction experienced hot spots. In Figure 3.14(c) the near-field is plotted for the normalized electric field in the zx-plane. The hot spots can be seen at the corners of the nanoprism. It can be observed that the natural near-field pattern is disturbed by the substrate and a part fo the near-field plot is observed inside the substrate. Figure 3.14(d) indicates the electric field component E_x in the xy-plane.

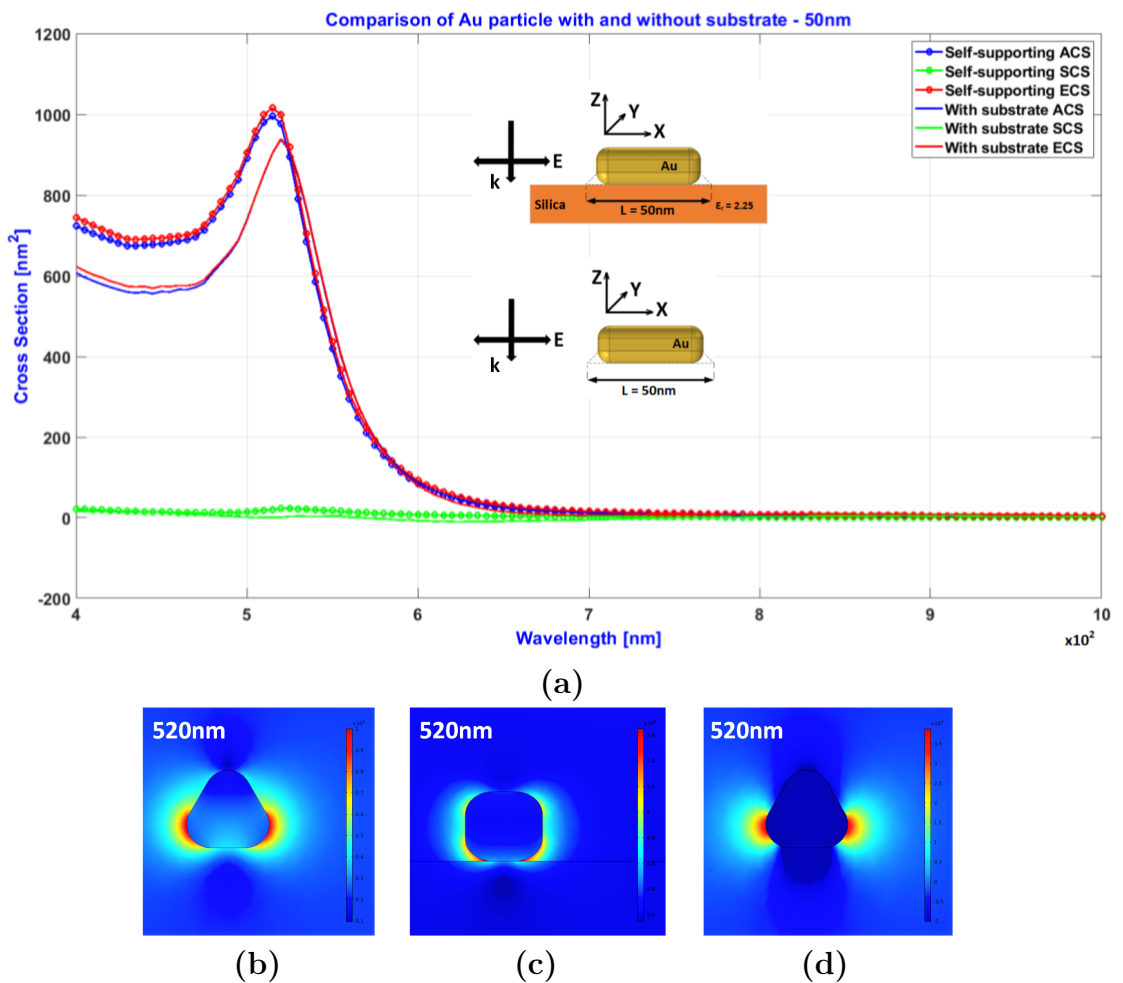


Figure 3.14.: (a)Comparison of cross-section parameters for with and without substrate models, length: 50nm, (b) near-field plot of normalized electric field in xy-plane, (c) near-field plot of normalized electric field in xz-plane, (d) electric field component E_x in xy-plane

Au nanoprism(Length 75nm) on substrate

From Figure 3.15(a) it can be observed that there is a small shift in the resonant frequency of 20nm from 535nm for self-supporting Au nanoprism model to 555nm for the Au nanoprism with substrate model of length 75nm. This shift in frequency depicts the effect of substrate on the Au particle. Near-field plot in Figure 3.15(b) shows normalized electric field in xy-plane with strong hot spots on the corners of the nanoprism. Only the sides which are along the polarization direction experienced hot spots. In Figure 3.15(c) the near-field is plotted for the normalized electric field in the zx-plane. The hot spots can be seen at the corners of the nanoprism. It can be observed that the natural near-field pattern is disturbed by the substrate and a part fo the near-field plot is observed inside the substrate. Figure 3.15(d) indicates the electric field component E_x in the xy-plane.

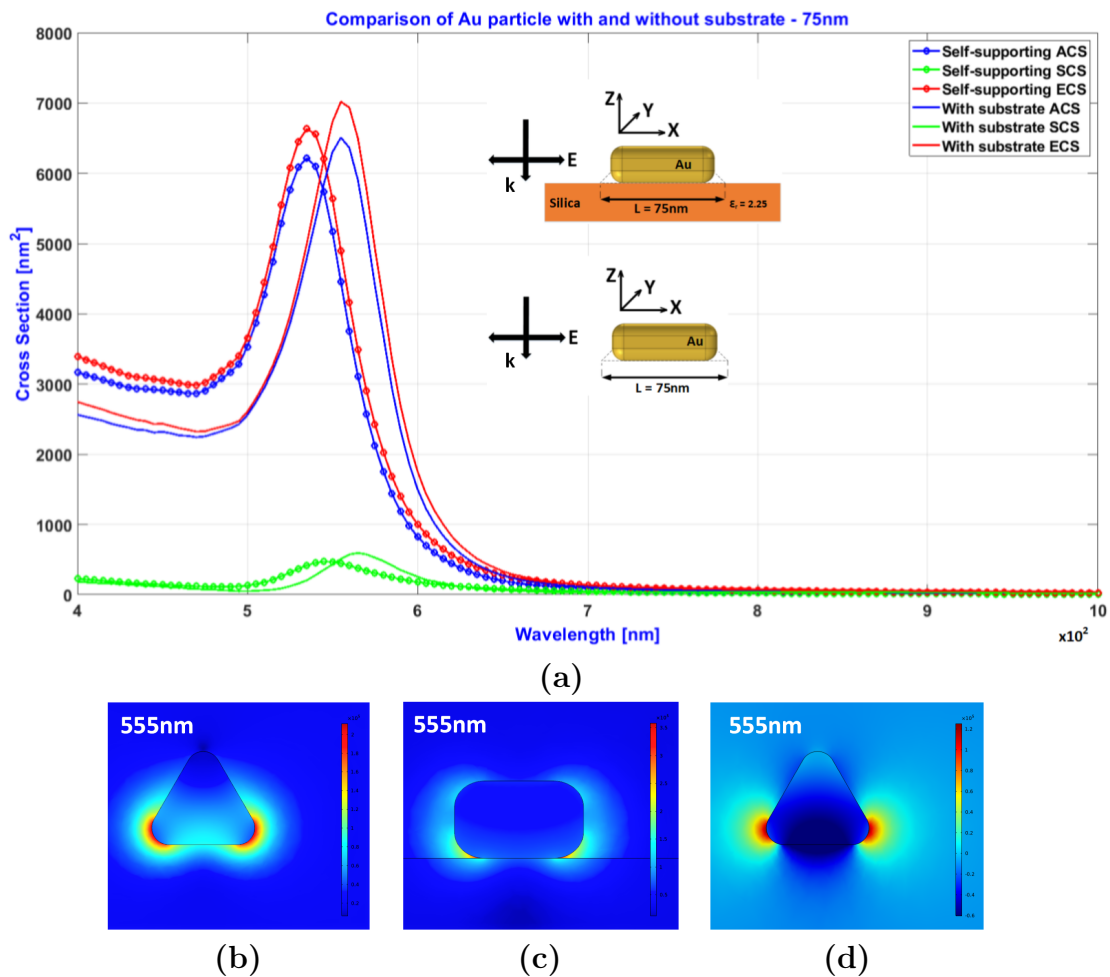


Figure 3.15.: (a)Comparison of cross-section parameters for with and without substrate models, length: 75nm, (b) near-field plot of normalized electric field in xy-plane, (c) near-field plot of normalized electric field in xz-plane, (d) electric field component E_x in xy-plane

Au nanoprism(Length 100nm) on substrate

From Figure 3.16(a) it can be observed that there is a small shift in the resonant frequency of 35nm from 565nm for self-supporting Au nanoprism model to 600nm for the Au nanoprism with substrate model of length 100nm. This shift in frequency depicts the effect of substrate on the Au particle. Near-field plot in Figure 3.16(b) shows normalized electric field in xy-plane with strong hot spots on the corners of the nanoprism. Only the sides which are along the polarization direction experienced hot spots. In Figure 3.16(c) the near-field is plotted for the normalized electric field in the zx-plane. The hot spots can be seen at the corners of the nanoprism. It can be observed that the natural near-field pattern is disturbed by the substrate and a part fo the near-field plot is observed inside the substrate. Figure 3.16(d) indicates the electric field component E_x in the xy-plane.

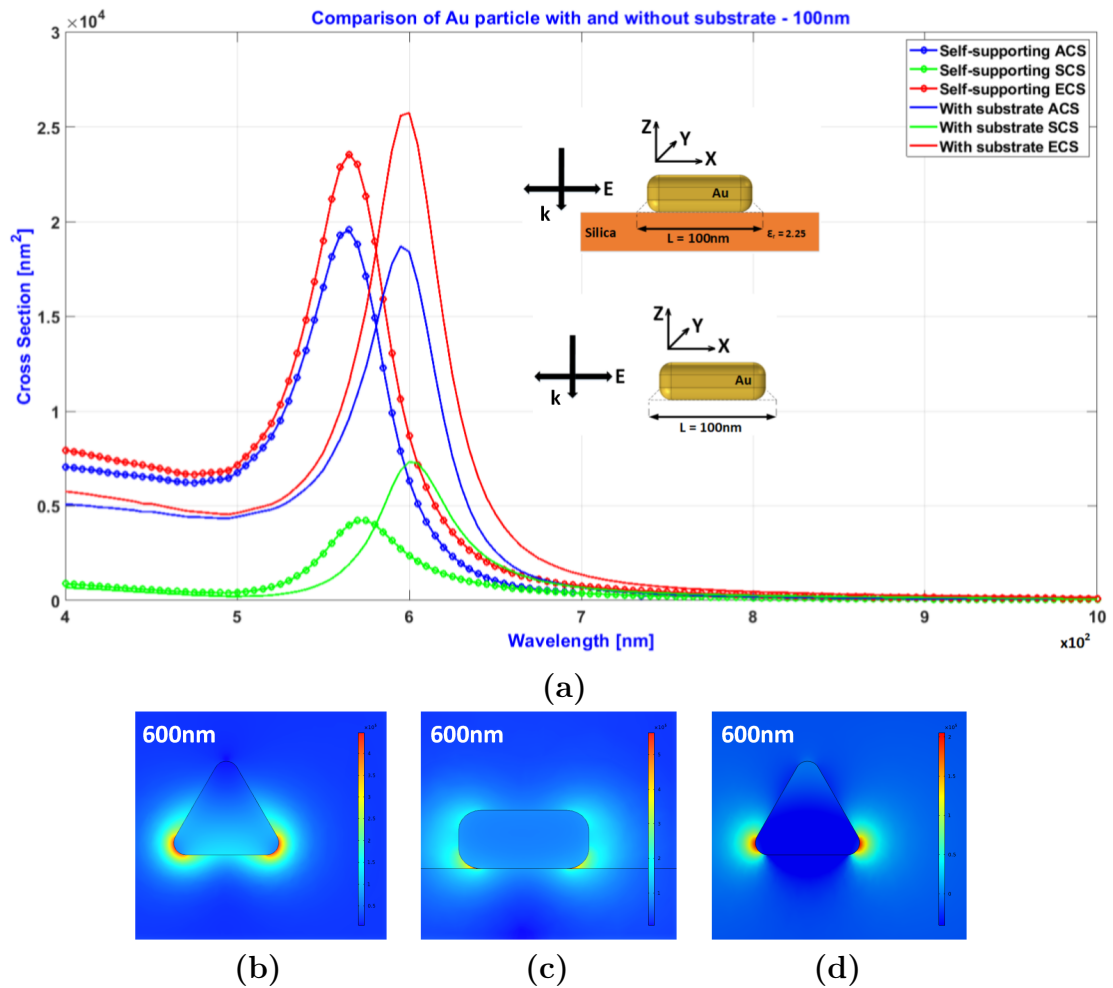


Figure 3.16.: (a)Comparison of cross-section parameters for with and without substrate models, length: 100nm, (b) near-field plot of normalized electric field in xy-plane, (c) near-field plot of normalized electric field in xz-plane, (d) electric field component E_x in xy-plane

Gold nanoprism(Length 150nm) on substrate

From Figure 3.17(a) it can be observed that there is a small shift in the resonant frequency of 65nm from 630nm for self-supporting Au nanoprism model to 695nm for the Au nanoprism with substrate model of length 150nm. This shift in frequency depicts the effect of substrate on the Au particle. Near-field plot in Figure 3.17(b) shows normalized electric field in xy-plane with strong hot spots on the corners of the nanoprism. Only the sides which are along the polarization direction experienced hot spots. In Figure 3.17(c) the near-field is plotted for the normalized electric field in the zx-plane. The hot spots can be seen at the corners of the nanoprism. It can be observed that the natural near-field pattern is disturbed by the substrate and a part fo the near-field plot is observed inside the substrate. Figure 3.17(d) indicates the electric field component E_x in the xy-plane.

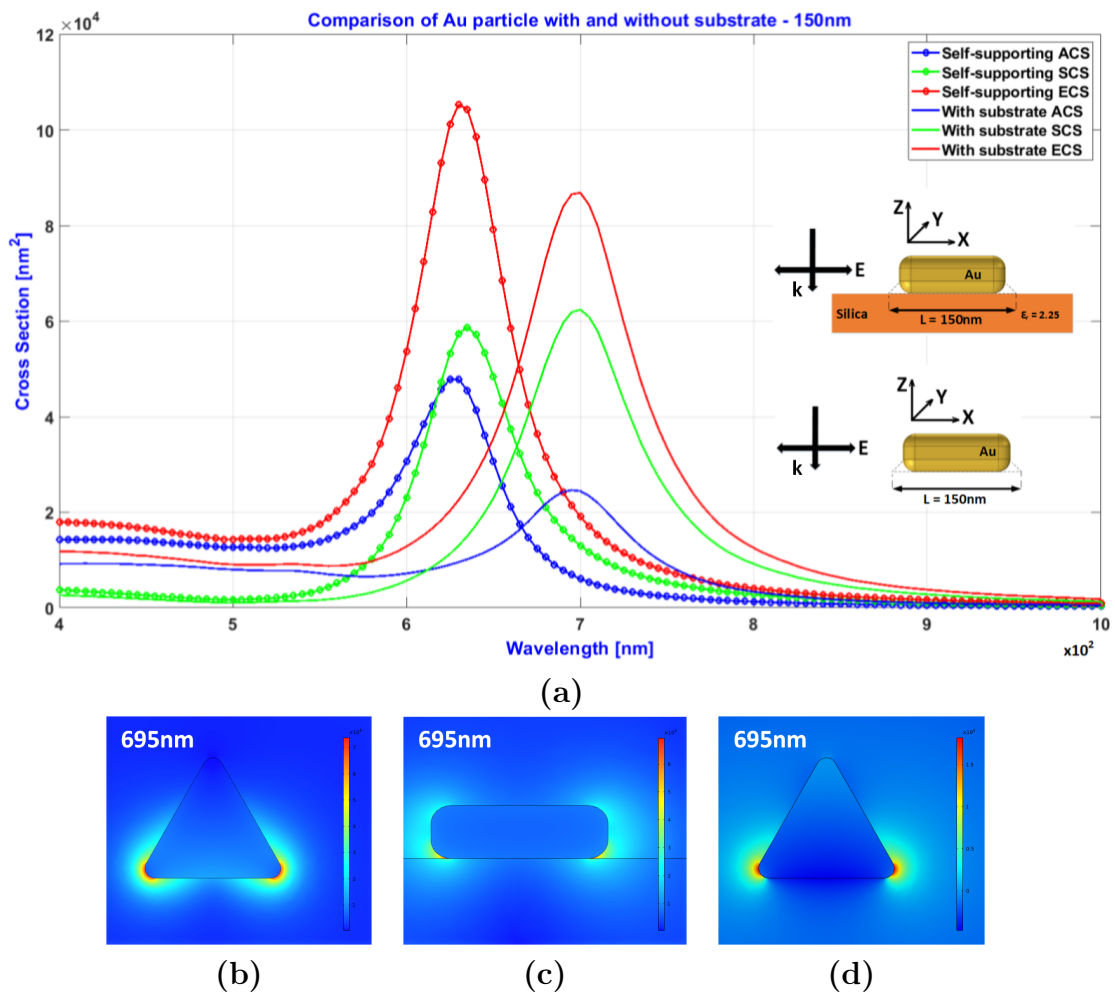


Figure 3.17.: (a)Comparison of cross-section parameters for with and without substrate models, length: 150nm, (b) near-field plot of normalized electric field in xy-plane, (c) near-field plot of normalized electric field in xz-plane, (d) electric field component E_x in xy-plane

Gold nanoprism(Length 200nm) on substrate

From Figure 3.18(a) it can be observed that there is a small shift in the resonant frequency of 105nm from 710nm for self-supporting Au nanoprism model to 815nm for the Au nanoprism with substrate model of length 200nm. A weak quadrupolar resonance can be seen at 550nm. This shift in frequency depicts the effect of substrate on the Au particle. Near-field plot in Figure 3.18(b) shows normalized electric field in xy-plane with strong hot spots on the corners of the nanoprism for dipolar resonance. Only the sides which are along the polarization direction experienced hot spots.

In Figure 3.18(c) the near-field is plotted for the normalized electric field in the zx-plane for dipolar resonance. The hot spots can be seen at the corners of the nanoprism. It can be observed that the natural near-field pattern is disturbed by the substrate and a part fo the near-field plot is observed inside the substrate. Figure 3.18(d) indicates the electric field component E_x in the xy-plane for dipolar resonance.

Figure 3.18(e) shows near-field plot of normalized electric field in xy-plane with strong hot spots on the sides of the nanoprism for the quadrupolar resonance. Unlike the dipolar resonance, the quadrupolar resonance near-field hot spots are on the sides of the nanoprism. In Figure 3.18(f) the near-field is plotted for the normalized electric field in the zx-plane for quadrupolar resonance. The hot spots can be seen at the corners of the nanoprism. It can be observed that the natural near-field pattern is disturbed by the substrate and a part of the near-field plot is observed inside the substrate. Figure 3.18(g) indicates the electric field component E_x in the xy-plane for quadrupolar resonance.

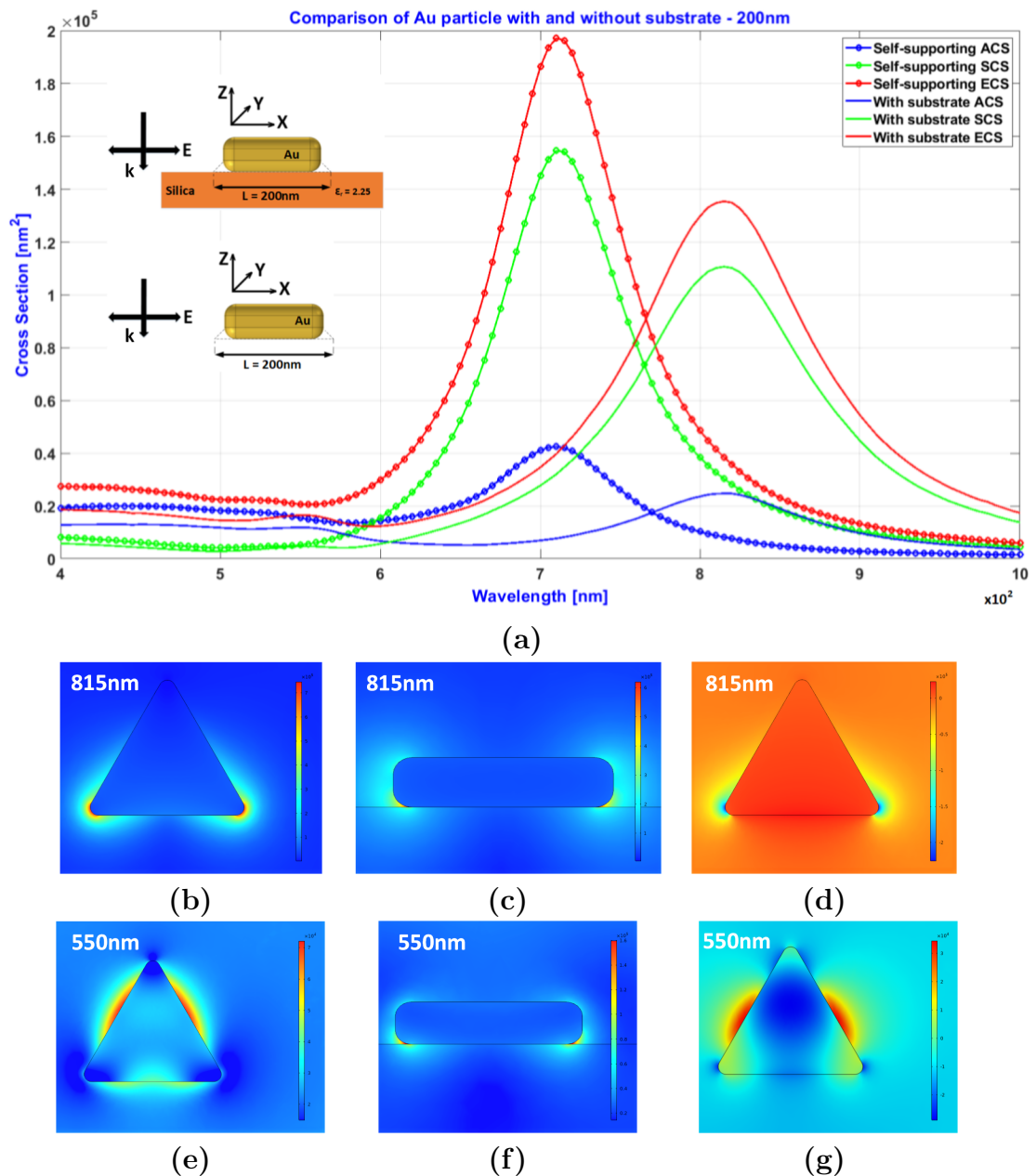


Figure 3.18.: (a)Comparison of cross-section parameters for with and without substrate models, length: 200nm; dipolar resonance: (b) near-field plot of normalized electric field in xy-plane, (c) near-field plot of normalized electric field in xz-plane, (d) electric field component E_x in xy-plane; quadrupolar resonance: (e) near-field plot of normalized electric field in xy-plane, (f) near-field plot of normalized electric field in xz-plane, (g) electric field component E_x in xy-plane

Gold nanoprism(Length 250nm) on substrate

From Figure 3.19(a) it can be observed that there is a small shift in the resonant frequency of 135nm from 800nm for self-supporting Au nanoprism model to 935nm

for the Au nanoprism with substrate model of length 250nm. A quadrupolar resonance can be seen shifting from 545nm to 585nm. This shift in frequency depicts the effect of substrate on the Au particle.

Near-field plot in Figure 3.19(b) shows normalized electric field in xy-plane with strong hot spots on the corners of the nanoprism for dipolar resonance. Only the sides which are along the polarization direction experienced hot spots. In Figure 3.19(c) the near-field is plotted for the normalized electric field in the zx-plane for dipolar resonance. The hot spots can be seen at the corners of the nanoprism. It can be observed that the natural near-field pattern is disturbed by the substrate and a part fo the near-field plot is observed inside the substrate. Figure 3.19(d) indicates the electric field component E_x in the xy-plane for dipolar resonance.

Figure 3.19(e) shows near-field plot of normalized electric field in xy-plane with strong hot spots on the sides of the nanoprism for the quadrupolar resonance. Unlike the dipolar resonance, the quadrupolar resonance near-field hot spots are on the sides of the nanoprism. In Figure 3.19(f) the near-field is plotted for the normalized electric field in the zx-plane for quadrupolar resonance. The hot spots can be seen at the corners of the nanoprism. It can be observed that the natural near-field pattern is disturbed by the substrate and a part of the near-field plot is observed inside the substrate. Figure 3.19(g) indicates the electric field component E_x in the xy-plane for quadrupolar resonance.

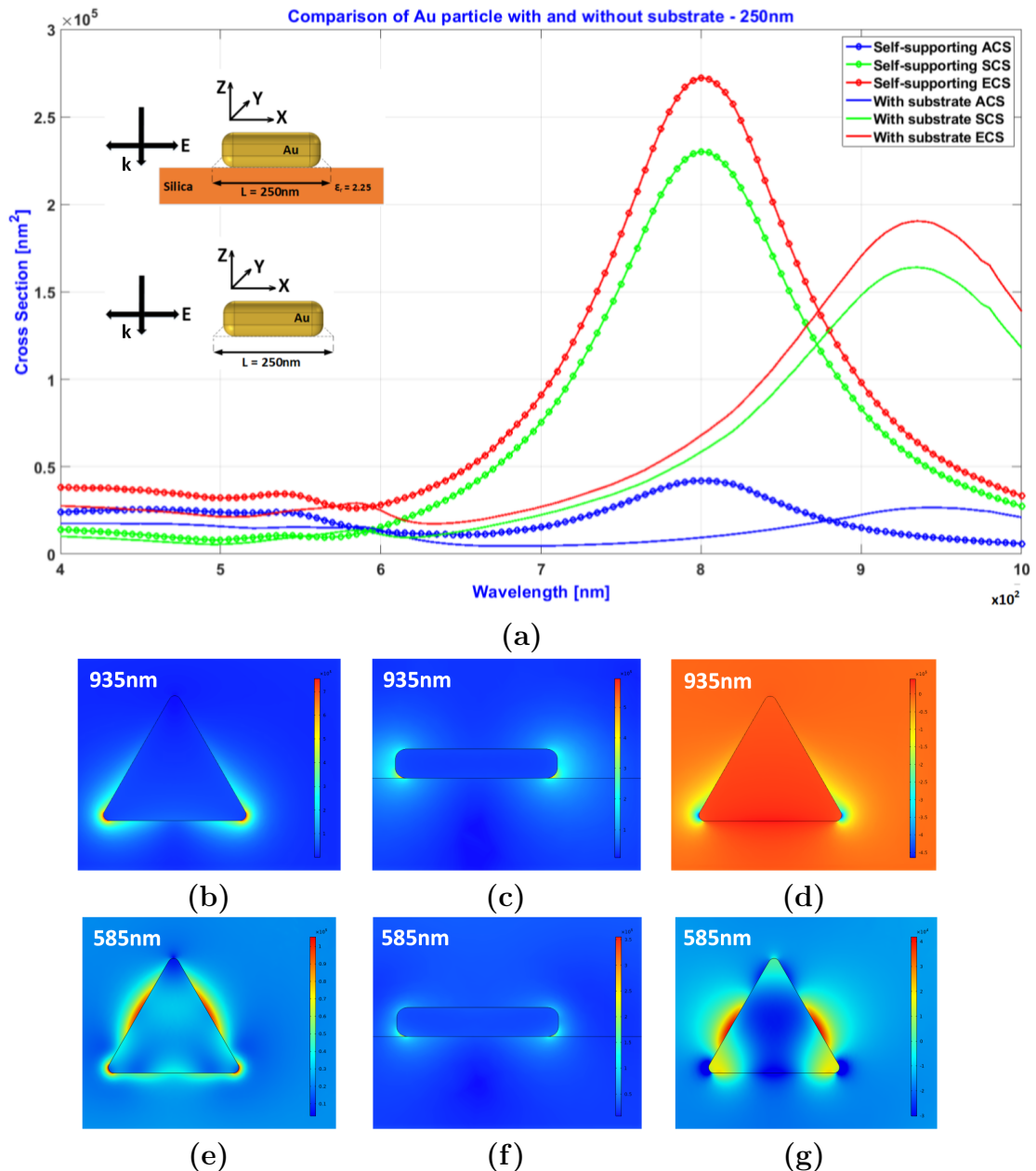


Figure 3.19.: (a)Comparison of cross-section parameters for with and without substrate models, length: 250nm; dipolar resonance: (b) near-field plot of normalized electric field in xy-plane, (c) near-field plot of normalized electric field in xz-plane, (d) electric field component E_x in xy-plane; quadrupolar resonance: (e) near-field plot of normalized electric field in xy-plane, (f) near-field plot of normalized electric field in xz-plane, (g) electric field component E_x in xy-plane

3.4. Absorption Cross-Section Vs Scattering Cross-Section

Figures 3.20(a) and 3.20(b) show the plots of ACS and SCS for different sizes of self-supporting of Au nanoprism. From the ACS plot it can be seen that ACS magnitude increased from Au particle of lengths 50nm to 150nm and started declining. The SCS magnitude in the SCS plot kept increasing exponentially. From the two plots it can be concluded that below 150nm size, the Au nanoprism is absorbing more excited field than scattering. From 150nm the Au nanoprism surface is large enough for the scattering to take over the absorption cross-section by a larger magnitude. In Figures 3.20(c) and 3.20(d) a similar effect can be seen for the Au nanoprism with substrate. But in the ACS plot of Figures 3.20(c) it can be seen that after 150nm size, the absorption is increasing by smaller magnitude instead of decreasing. This slight increase is the effect of dielectric substrate.

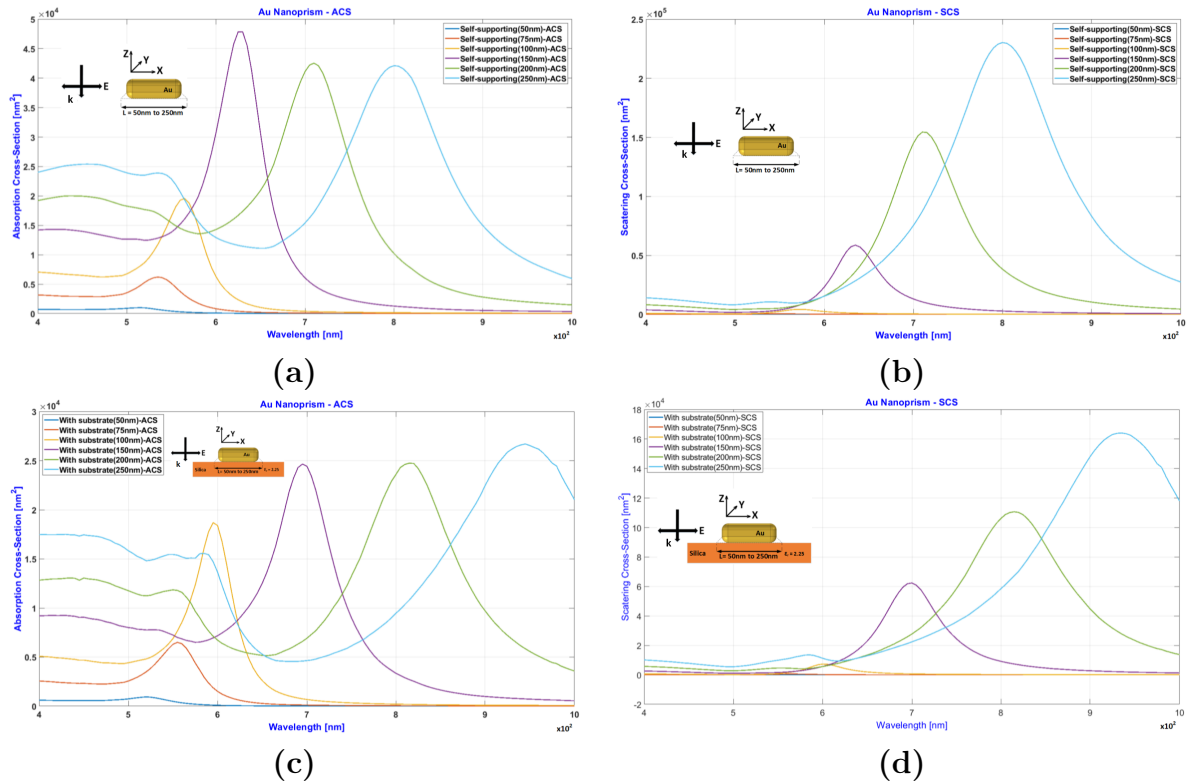


Figure 3.20.: Self-supporting Au nanoprism: (a)ACS for different sizes of Self-supporting Au nanoprism, (b) SCS for different sizes of Self-supporting Au nanoprism; Au nanoprism with substrate: (c) ACS for different sizes of Au nanoprism with substrate, (d) SCS for different sizes of Au nanoprism with substrate

3.5. Effect of substrate on the resonant frequency

Figure 3.21 plotted for the resonant frequency values of the two models against the size of the particle. It can be observed that when the nanoprism size is very small the shift in resonant frequency is small. As the nanoprism size increases the shift in the frequency increases by a larger magnitude.

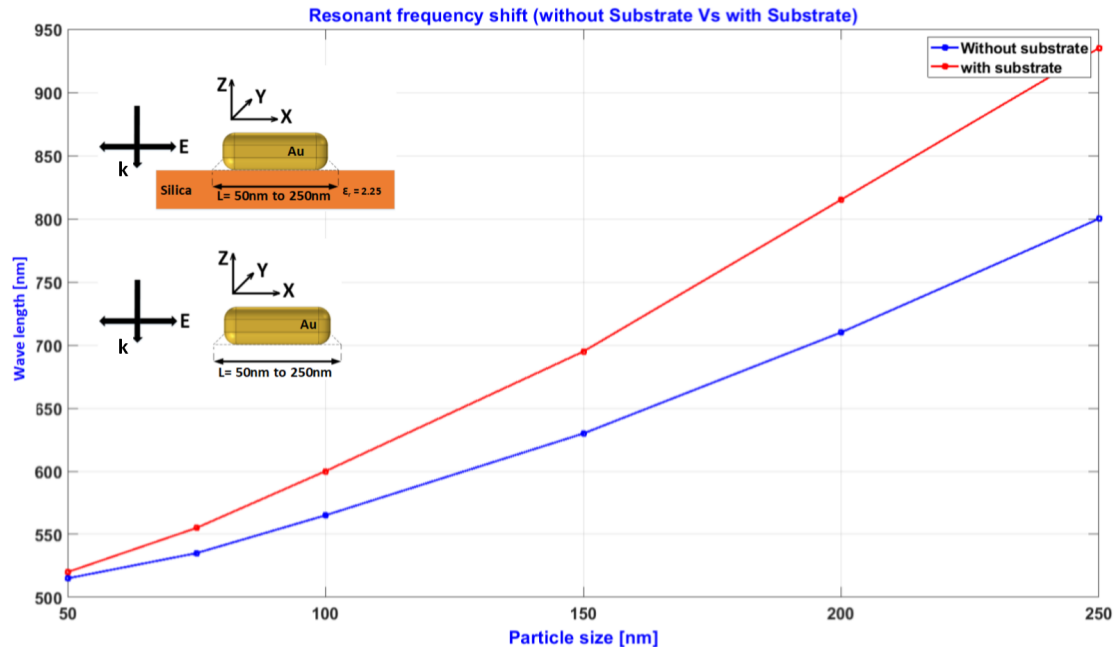


Figure 3.21.: Effect of substrate on resonant frequency of Au nanoprism of different sizes

4. Conclusion and Future work

We have successfully modeled a self-supporting Au nanoprism and calculated the optical cross-section parameters in frequency domain as a function of the nanoprism size between 50nm and 250nm side length. The incident plane wave on this model is propagating in negative z-direction and polarizing in x-direction. We have explained each nanoparticle with respect to their cross-section parameters, near-field radiation, far-field radiation and electric field component along x-direction. We have also explained the different methods of calculating SCS and showed that both the methods give same results. From the optical cross-section plots we observed that the nanoprism absorbs more radiation compared to scattering at smaller sizes of the nanoprism. When the nanoprism reaches 150nm side length the scattering is larger than absorption and the gap between them increases as the nanoprism size increases.

We have also modeled Au nanoprism on a semi-infinite silica substrate and calculated the optical cross-section parameters in frequency domain as a function of the nanoprism size between 50nm and 250nm side length similar to self-supporting Au nanoprism model. We used two different plane waves one with propagation in negative z-direction and polarization in x-direction and other with propagation in negative z-direction and polarization in y-direction. We found out that when this model is excited using these two plane waves individually, the Au nanoprism experiences degenerate mode where both planes cause same resonance frequencies.

We then compared the two models with respect to optical cross-section parameters and observed that for smaller nanoprisms the shift in the resonance frequency due to the presence of substrate is small and as the nanoprism size increases the shift in the resonance frequency increases exponentially.

As future work, we leave the idea of modeling two triangular Au nanoprisms facing each other separated by a small distance and study their optical and electromagnetic properties. The semi-infinite dielectric substrate in the model 2 can be replaced by different shapes, sizes and materials, study their effects on the optical cross-section parameters of the Au triangular nanoprism. The above mentioned ideas along with the two models presented in this project can be studied by varying the angles of propagation and polarization of the plane wave.

A. Appendix

List of Acronyms

ACS Absorption Cross-Section

SCS Scattering Cross-Section

ECS Extinction Cross-Section

PML Perfectly Matched Layer

Au Aurum

EM Electromagnetic

CNT carbon nanotubes

LSPR Localized Surface Plasmon Resonance

LSP Localized Surface Plasmon

UV ultraviolet

SPR surface plasmon resonance

SPP surface plasmon polariton

FEM Finite Element Method

PDE partial differential equations

EM electromagnetic field

Bibliography

- [1] Sophie Laurent, Delphine Forge, Marc Port, Alain Roch, Caroline Robic, Luce Vander Elst, and Robert N. Muller. *"Magnetic Iron Oxide Nanoparticles: Synthesis, Stabilization, Vectorization, Physicochemical Characterizations, and Biological Applications"*. American Chemical Society, 04 2010.
- [2] Jitendra Tiwari, Rajanish Tiwari, and Kwang Kim. *"Zero-dimensional, one-dimensional, two-dimensional and three-dimensional nanostructured materials for advanced electrochemical energy devices"*. *Progress in Materials Science*, 57:724–803, 05 2012.
- [3] Erik C. Dreaden, Alaaldin M. Alkilany, Xiaohua Huang, Catherine J. Murphy, and Mostafa A. El-Sayed. *"The golden age: gold nanoparticles for biomedicine"*. *Chem. Soc. Rev.*, 41:2740–2779, 2012.
- [4] Khalid Saeed Ibrahim. *"Carbon nanotubes-properties and applications: a review"*. *Carbon letters*, 14(3):131–144, 07 2013.
- [5] Alina Astefanei, Oscar Núñez, and Maria Teresa Galceran. *"Characterisation and determination of fullerenes: A critical review"*. *Analytica Chimica Acta*, 882:1–2, 03 2015.
- [6] Shindu Thomas, Harshita Sharma, Pawan Mishra, and Sushama Talegaonkar. *"Ceramic Nanoparticles: Fabrication Methods and Applications in Drug Delivery"*. *Current pharmaceutical design*, 21, 10 2015.
- [7] Shahid Ali, Ibrahim Khan, Safyan Khan, Manzar Sohail, Riaz Ahmed, Ateeq Rehman, Muhammad Shahid Ansari, and Mohamed Morsy. *"Electrocatalytic performance of Ni@Pt core-shell nanoparticles supported on carbon nanotubes for methanol oxidation reaction"*. *Journal of Electroanalytical Chemistry*, 795:17–25, 04 2017.
- [8] Abd Ellah and Abouelmagd. *"Surface functionalization of polymeric nanoparticles for tumor drug delivery: approaches and challenges"*. *Expert Opinion on Drug Delivery*, 24(3-4):475–487, 2003.
- [9] Sara A. Abouelmagd, Fanfei Meng, Bieong-Kil Kim, Hyesun Hyun, and Yoon Yeo. *"Tannic Acid-Mediated Surface Functionalization of Polymeric Nanoparticles"*. *ACS Biomaterials Science & Engineering*, 2(12):2294–2303, 2016.
- [10] Ibrahim Khan, Khalid Saeed, and Idrees Khan. *"Nanoparticles: Properties, Applications and Toxicities"*. *Arabian Journal of Chemistry*, pages –, 05 2017.

- [11] Viktor Myroshnychenko, Jessica Rodríguez-Fernández, Isabel Pastoriza-Santos, Alison Funston, Carolina Novo, Paul Mulvaney, Luis Liz-Marzán, and Javier Garcia de Abajo. "Modeling the optical response of gold nanoparticles". *Chemical Society reviews*, 37:1792–805, 10 2008.
- [12] British Museum. "The Lycurgus Cup". <https://britishmuseum.tumblr.com/post/120689869617/the-lycurgus-cup>.
- [13] reddit user. "The Stained Glass of Sainte-Chapelle in Paris". https://www.reddit.com/r/travel/comments/8smwhx/the_stained_glass_of_saintechapelle_in_paris/.
- [14] Günter Reiss and Andreas Hütten. "Applications beyond data storage". *Nature Materials*, 4, 10 2005.
- [15] Hannah Kearney. "Plasmon Resonance". [https://eng.libretexts.org/Bookshelves/Materials_Science/Supplemental_Modules_\(Materials_Science\)/Semiconductors/Plasmon_Resonance](https://eng.libretexts.org/Bookshelves/Materials_Science/Supplemental_Modules_(Materials_Science)/Semiconductors/Plasmon_Resonance).
- [16] Anatoly Zayats, Igor Smolyaninov, and Alexei Maradudin. "Nano-Optics of surface plasmon polaritons". *Physics Reports* 001 132 A.V. Zayats et al. *Physics Reports*, 4082011:131–314, 03 2005.
- [17] William L. Barnes, Alain Dereux, and Thomas W. Ebbesen. "Surface Plasmon Subwavelength Optics". *Nature*, 424:824–830, 08 2003.
- [18] Christian Heck. "Gold and silver nanolenses self-assembled by DNA origami". PhD thesis, Universität Potsdam, 04 2018.
- [19] Xuetong Ci, Botao Wu, Min Song, Yan Liu, Gengxu Chen, Eddy wu, and Heping Zeng. "Tunable Fano resonances in heterogenous Al-Ag nanorod dimer". *Applied Physics A*, 117, 12 2013.
- [20] Bala's Website. "DDSCAT and electric field at plasmon resonance". <http://juluribk.com/2010/05/26/ddscat-and-electric-field-at-plasmon-resonance/>.
- [21] Jeffrey S. Crompton Sergei Yushanov and Kyle C. Koppenhoefer. "Mie Scattering of Electromagnetic Waves". https://www.comsol.com/paper/download/181101/crompton_paper.pdf.
- [22] Prashant Jain, Ivan El-Sayed, and Mostafa El-Sayed. "Au Nanoparticles Target Cancer". *Nano Today*, 2:18–29, 02 2007.
- [23] NS Barakat, DAB Taleb, and Al Salehi AS. "Target Nanoparticles: An Appealing Drug Delivery Platform". *Journal of Nanomedicine & Nanotechnology*, 03 2012.

- [24] Scott Jung. "*Flexible, Advanced Sensor Could Lead to Ultra-Sensitive Artificial Skin*". <https://www.medgadget.com/2013/07/technion-israel-institute-of-technology-artificial-skin.html>.
- [25] Research Group. "*Application of Nanotechnology in Food Science and Food Microbiology*". <https://www.frontiersin.org/research-topics/5194/application-of-nanotechnology-in-food-science-and-food-microbiology>.
- [26] Axelevitch A, Gorenstein B, and Golan G. "*Application of gold nano-particles for silicon solar cells efficiency increase*". *Applied Surface Science*, 315:523–526, 2014.
- [27] COMSOL.de. "*The Finite Element Method (FEM)*". <https://www.comsol.de/multiphysics/finite-element-method>.
- [28] Inc. COMSOL.com. Comsol. "*COMSOL Modeling Software*". <https://www.comsol.com/release/5.4>.
- [29] Dr. P. Venkataraman. "*An Introduction to COMSOL*". <https://people.rit.edu/pnveme/personal/VenkatCOMSOL42/IntroductionCOMSOL/index.html>.
- [30] "*Finite Element Method Procedure in COMSOL Multiphysics*". <http://www.iue.tuwien.ac.at/phd/rovitto/node/72.html>.
- [31] COMSOL. "*RF Module User Guide*". <https://is.muni.cz/el/1431/podzim2013/F7061/um/RFModuleUsersGuide.pdf>.
- [32] Peter B. Johnson and R W. Christy. "*Optical Constants of Noble Metals*". *Physical Review B*, 6, 12 1972.
- [33] COMSOL. "*Scatter on Substrate*". <https://www.comsol.com/model/scatterer-on-substrate-14699>.

